

On Relative Pose Recovery for Multi-Camera Systems

Ji Zhao and Banglei Guan

Abstract—The point correspondence (PC) and affine correspondence (AC) are widely used for relative pose estimation. An AC consists of a PC across two views and an affine transformation between the small patches around this PC. Previous work demonstrates that one AC generally provides three independent constraints for relative pose estimation. For multi-camera systems, there is still not any AC-based minimal solver for general relative pose estimation. To deal with this problem, we propose a complete solution to relative pose estimation from two ACs for multi-camera systems, consisting of a series of minimal solvers. The solver generation in our solution is based on Cayley or quaternion parameterization for rotation and hidden variable technique to eliminate translation. This solver generation method is also naturally applied to relative pose estimation from PCs, resulting in a new six-point method for multi-camera systems. A few extensions are made, including relative pose estimation with known rotation angle and/or with unknown focal lengths. Extensive experiments demonstrate that the proposed AC-based solvers and PC-based solvers are effective and efficient on synthetic and real-world datasets.

Index Terms—Relative pose estimation, minimal solver, multi-camera system, affine correspondence, point correspondence, two view geometry, epipolar geometry



1 INTRODUCTION

ESTIMATING the relative pose of images given feature correspondences is one foundational task in geometric vision. It is crucial for many popular tasks, such as structure-from-motion, simultaneous localization and mapping, autonomous driving, augmented reality, etc. Despite its long history, relative pose estimation is still an active research area. A lot of methods have been developed to improve its accuracy, efficiency, numerical stability, and robustness.

Camera models play an important role in relative pose estimation. While a single camera can be modeled by a pinhole or perspective camera model [1], more complicated cameras such as multi-camera systems should be modeled by the generalized camera model [2]. A generalized camera is formed by abstracting landmark observations into spatial rays that are no longer required to originate from a common point (i.e., the focal point). This paper deals with both a single camera and a multi-camera rig of rigidly attached cameras. Multi-camera systems are popular in autonomous driving [3] and many robotic applications. It is well-known that the standard epipolar geometry exists an unobservability in the scale of the translation [1]. In contrast, the scale of translation estimated for a multi-camera system is generally unique. The down-side of this scale observability is that the minimal solution of the relative pose requires at least 6 instead of only 5 point correspondences (PCs) across the two views.

Since feature correspondences inevitably contain outliers, a robust estimator should be applied to recover the

correct pose and remove outliers. In computer vision and robotics communities, the most popular framework is random sample consensus (RANSAC) [4] and its variants. The core component in RANSAC is a minimal solver. Minimal solvers for relative pose estimation usually rely on PCs. According to the well-known epipolar geometry, each PC provides one constraint for a relative pose. For single cameras, the representative methods for relative pose estimation are called five-point methods [5], [6], [7], [8], [9], [10]. For multi-camera systems, the development of minimal solvers for relative pose estimation ranges back to the six-point method [11]. Later, many other works have been subsequently proposed, such as the 17-point linear solvers [12], an efficient solver based on iterative optimization [13], and a solver based on global optimization [14].

The efficiency of RANSAC depends on the runtime of the minimal solver and iteration number. Using fewer feature correspondences in minimal solvers will cause fewer iterations. Thus much effort has been made to reduce the required number of feature correspondences in minimal solvers while keeping their efficiency. In recent years, there are a series of work exploiting affine correspondences (ACs) to estimate relative pose [15], [16], [17], [18], [19], [20]. Since one AC provides more independent constraints than one PC, fewer ACs than PCs are needed to solve pose estimation problems. Several minimal solvers using ACs have been developed for different tasks. For single cameras, there are pose estimation methods for general 5 degrees of freedom (DOF) motion [17], 3DOF motion with known rotation axis [21], and 2DOF motion with planar motion [21], [22]. For multi-camera systems, there are pose estimation methods for motion with known rotation axis and planar motion [23].

This paper mainly deals with the full DOF relative pose estimation for multi-camera systems, see Fig. 1. Due to

- J. Zhao is in Beijing, China.
E-mail: zhaoji84@gmail.com
- B. Guan is with College of Aerospace Science and Engineering, National University of Defense Technology, Changsha 410073, China.
E-mail: guanbanglei12@nudt.edu.cn

(Corresponding author: Ji Zhao)

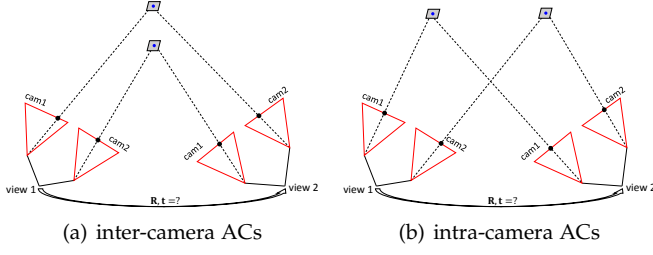


Fig. 1. Relative pose estimation from ACs for a multi-camera system. Two oriented points (or infinitesimal patches equivalently) are captured by two views of a two-camera rig. We aim to recover the 6DOF relative pose using two ACs.

the diversity of camera layout for multi-camera systems, the minimal solvers are complicated. Fig. 1 demonstrates the relative pose estimation from inter-camera ACs and intra-camera ACs. The corresponding solvers for these two configurations are different. In this paper, the proposed AC-based minimal solvers form a complete solution to relative pose estimation for multi-camera systems. We also demonstrated that our method is versatile to be applied to PCs and many extensions straightforwardly. The contributions of this paper are three-fold.

- We mainly deal with full DOF relative pose estimation from ACs for multi-camera systems. A series of minimal solvers are proposed, which cover all camera layouts and AC types of this problem. The proposed minimal solvers form a complete solution to this problem. To the best of our knowledge, this is the first solution that can provide minimal solvers to this problem.
- Using the same equation system construction and solver generation, two minimal solvers are proposed for full DOF relative pose estimation from PCs. They are new six-point methods for popular configurations of two-camera rigs.
- Our solver generation is based on a unified and versatile framework, which exploits Cayley or quaternion parameterization for rotation and uses the hidden variable technique to eliminate translation. We proved that a factor should be factored out to avoid false roots and simplify the equation system. This framework has broad applications in relative pose estimation. In the supplementary material, some minimal solvers are generated with a known rotation angle and/or unknown focal lengths.

The paper is organized as follows. Section 2 introduces the related work. In Section 3, minimal configurations and degenerate cases for relative pose estimation from ACs are figured out. For both single cameras and multi-camera systems, Section 4 proposes a complete solution and a series of AC-based minimal solvers for relative pose estimation. A few PC-based minimal solvers for multi-camera systems are provided in Section 5. Section 6 presents the performance of our method in comparison to other methods, followed by a concluding discussion in Section 7.

2 RELATED WORK

Relative pose estimation is an essential topic in computer vision, and there are many methods in this area. We introduce

a taxonomy of these methods along four independent axes.

First, relative pose estimation methods can be applied for single cameras [5], [6], [7], [8], [9], [10], multi-camera systems or generalized cameras [11], [12], [13], [14]. Moreover, the cameras include fully calibrated cameras and partially calibrated cameras with unknown focal length and/or radial distortion.

Second, the exploited geometric primitives can be points [5], [11], oriented points [15], [16], hybrid of point and line structures [24], [25], [26], etc. Recently, oriented points (or an infinitesimal patch equivalently) have drawn much attention. The images of an oriented point captured by different views form an AC between affine-covariant features. One AC provides a 2×2 affine transformation matrix between the local patches around the corresponding points in two images. Two-view geometry of AC has been investigated [15], [16], [18], [19], and several methods of relative pose from ACs has been proposed [15], [16], [17], [18], [19], [20]. In addition, there are relative pose estimation methods [27], [28], [29] exploit orientation- and scale-covariant features obtained by e.g. the SIFT detector [30].

Third, a relative pose estimation method can be classified as a minimal solver [5], [11], a non-minimal solver [13], [14], [31], [32] or a linear solver [12], [33]. Minimal solvers use the minimum required number of geometric primitives to estimate relative pose. Non-minimal solvers use all correct correspondences to estimate an accurate relative pose. The linear solvers also use larger-than-minimal correspondences, but their primary purpose is finding a simple and efficient solution. Linear solvers usually ignore certain implicit constraints for unknowns to gain efficiency. In contrast, minimal solvers and non-minimal solvers consider all the implicit constraints for unknowns. This paper focuses on minimal solvers.

Fourth, existing methods might estimate the pose with or without a prior. One popular scene prior is the planar assumption. If 3D points lie on a plane, the relative pose can be recovered by estimating homography using 4 PCs [1] or 1AC+1PC [34]. Usually, the pose priors include known rotation axis prior, known rotation angle prior, planar motion prior, or Ackermann motion prior. Common ways to obtain the directional direction are given by vanishing point estimation or sensor fusion with an inertial measurement unit (IMU) to measure the direction of gravity. The known rotation axis prior can reduce the DOF of rotation by two [35], [36], [37], [38], [39], [40]. The known rotation angle prior comes from a camera-IMU module with unknown extrinsic parameters, which reduces the DOF of rotation by one [41], [42], [43]. The planar motion prior can reduce the DOF of rotation and translation by two and one, respectively [44]. The Ackermann motion prior reduces the DOF to one for a single camera [45] and two for a multi-camera system [46]. In addition, there is a small-rotation prior. In this case, the rotation can be approximated by its first-order approximation [47].

The combination of the four aspects mentioned above produces many subcategories. Providing a comprehensive survey is beyond the scope of this paper. In the following text, we focus on four subcategories from the combination of two camera types (single camera or multi-camera system) and two correspondence types (PC or AC).

Single camera and PCs: Usually, five PCs are enough to estimate the relative pose of a single camera. In addition to the well-known five-point method [5], there are many other five-point methods, such as [6], [7], [8], [9], [10]. There are a lot of solvers with motion priors, such as known rotation axis [35], [37], [38], known axis angle [41], [42], [43], planar motion [44], and Ackermann motion [45]. If the camera is uncalibrated, there are some solvers that simultaneously estimate pose and intrinsic parameters, such as focal length [9], [48], [49], [50] and/or radial distortion [50], [51], [52].

Single camera and ACs: One AC usually provides 3 independent constraints on relative pose [15]. As a result, two ACs are enough to determine the relative pose for a single camera [16], [18], [19] or a single camera with unknown focal length [17]. In [20], guidelines are proposed for effective usage of ACs in the course of a full model estimation pipeline. When the relative pose has a motion prior, there are simple and efficient solvers. For example, there are many customized solvers when the rotation axis is known [21], the motion is under planar motion [21], [22], or the depth of feature points is known [53].

Multi-camera system and PCs: The first minimal solver for multi-camera systems was proposed in [11], which uses 6 PCs to estimate the relative pose. A linear solver that takes 17 PCs was proposed in [12]. Some solvers are developed in the context of structure-from-motion with special configurations [54], [55]. There are a few non-minimal solvers, which use local optimization [13] or global optimization method [14] to find the optimal relative poses. There are also solvers with motion priors, such as known rotation axis [36], [37], [56], a known rotation angle [43], and Ackermann motion [46]. A first-order approximation to relative pose was used in [47] to obtain an efficient solver.

Multi-camera system and ACs: Using ACs to estimate the relative pose of multi-camera systems is a relatively new research area. For non-degenerate cases, 2 ACs are enough for 6DOF pose estimation. A linear solution using 6 ACs was proposed in [57], which generalizes the 17-point solver for PCs [12]. Two minimal solvers were proposed for motion with known vertical direction or planar motion [23].

3 MINIMAL CONFIGURATIONS FOR POSE ESTIMATION FROM AFFINE CORRESPONDENCES

In this section, the intrinsic and extrinsic parameters of multi-camera systems are assumed to be calibrated. Our purpose is to find all the minimal configurations for the relative pose estimation by using ACs.

3.1 Two-View Geometry for A Single Camera

Denote the k -th AC as $(\mathbf{x}_k, \mathbf{x}'_k, \mathbf{A}_k)$, where \mathbf{x}_k and \mathbf{x}'_k are the homogeneous coordinates in normalized image plane for the first and the second views, respectively. \mathbf{A}_k is a 2×2 local affine transformation, which relates the infinitesimal patches around \mathbf{x}_k and \mathbf{x}'_k [16]. Generally speaking, one AC provides three independent constraints: one is derived from the point correspondence $(\mathbf{x}_k, \mathbf{x}'_k)$, and two are derived from the affine transformation \mathbf{A}_k . Denote the relative rotation and translation from the first view to the second view as \mathbf{R} and \mathbf{t} , respectively.

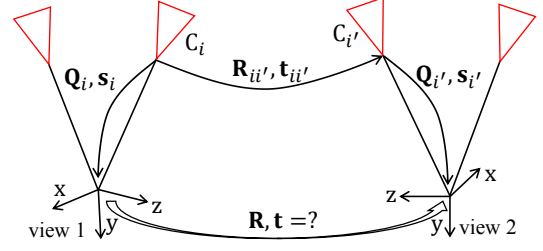


Fig. 2. Illustration of the relative pose estimation for a multi-camera system.

The constraint introduced by the point correspondence $(\mathbf{x}_k, \mathbf{x}'_k)$ is [1]

$$\mathbf{x}'_k{}^T \mathbf{E} \mathbf{x}_k = 0, \quad (1)$$

where

$$\mathbf{E} = [\mathbf{t}]_{\times} \mathbf{R}. \quad (2)$$

This constraint is the well-known epipolar constraint in two-view geometry. \mathbf{E} is known as the essential matrix.

The two constraints introduced by the affine transformation \mathbf{A} can be written as [18]

$$(\mathbf{E}^T \mathbf{x}'_k)_{(1:2)} + \mathbf{A}_k^T (\mathbf{E} \mathbf{x}_k)_{(1:2)} = 0, \quad (3)$$

where the subscript $(1:2)$ represents the first two entries of a vector.

3.2 Two-View Geometry for A Multi-Camera System

A multi-camera system is composed of several perspective cameras. Denote the extrinsic parameters of the i -th camera as $\{\mathbf{Q}_i, \mathbf{s}_i\}$. Here \mathbf{Q}_i and \mathbf{s}_i represent relative rotation and translation to the reference of the multi-camera system. Denote the relative rotation and translation from the first view to the second view of the multi-camera system as \mathbf{R} and \mathbf{t} , respectively.

An affine correspondence in a multi-camera system relates two perspective cameras across two views, see Fig. 2. Denote the k -th AC as $(\mathbf{x}_k, \mathbf{x}'_k, i_k, i'_k, \mathbf{A}_k)$. It means that an oriented point is captured by the i_k -th camera in the first view, and its homogeneous coordinate in the normalized image plane is \mathbf{x}_k . It is also captured by the i'_k -th camera in the second view, and its homogeneous coordinate is \mathbf{x}'_k . To simplify the notation, we omit the subscript k of camera indices i and i' in the following text.

If we consider cameras i and i' of an AC as one perspective camera across two views, the constraints of Eqs. (1) and (3) should still hold. However, the essential matrix \mathbf{E} , \mathbf{R} , and \mathbf{t} in these two equations should be newly defined. In addition, the essential matrices for different ACs are usually different. Specifically, the constraints introduced by the k -th AC are

$$\begin{cases} \mathbf{x}'_k{}^T \mathbf{E}_k \mathbf{x}_k = 0 \\ (\mathbf{E}_k^T \mathbf{x}'_k)_{(1:2)} + \mathbf{A}_k^T (\mathbf{E}_k \mathbf{x}_k)_{(1:2)} = 0 \end{cases} \quad (4a)$$

$$\quad (4b)$$

where

$$\mathbf{E}_k = [\mathbf{t}_{ii'}]_{\times} \mathbf{R}_{ii'}. \quad (5)$$

TABLE 1

Excess constraints for different configurations. There are n ACs across m views.

$n \backslash m$	1	2	3	4	5	6	7
1	-3	-6	-9	-12	-15	-18	-21
2	-3	0	3	6	9	12	15
3	-3	6	15	24	33	42	51
4	-3	12	27	42	57	72	87

$\{\mathbf{R}_{ii'}, \mathbf{t}_{ii'}\}$ is the relative pose from camera i in the first view to camera i' in the second view. It is determined by a composition of three transformations

$$\begin{aligned} \begin{bmatrix} \mathbf{R}_{ii'} & \mathbf{t}_{ii'} \\ \mathbf{0} & 1 \end{bmatrix} &= \begin{bmatrix} \mathbf{Q}_{i'} & \mathbf{s}_{i'} \\ \mathbf{0} & 1 \end{bmatrix}^{-1} \begin{bmatrix} \mathbf{R} & \mathbf{t} \\ \mathbf{0} & 1 \end{bmatrix} \begin{bmatrix} \mathbf{Q}_i & \mathbf{s}_i \\ \mathbf{0} & 1 \end{bmatrix} \\ &= \begin{bmatrix} \mathbf{Q}_{i'}^T \mathbf{R} \mathbf{Q}_i & \mathbf{Q}_{i'}^T (\mathbf{R} \mathbf{s}_i + \mathbf{t} - \mathbf{s}_{i'}) \\ \mathbf{0} & 1 \end{bmatrix}. \end{aligned} \quad (6)$$

By substituting $\mathbf{R}_{ii'}$ and $\mathbf{t}_{ii'}$ into Eq. (5), the essential matrix \mathbf{E}_k becomes

$$\begin{aligned} \mathbf{E}_k &= [\mathbf{Q}_{i'}^T (\mathbf{R} \mathbf{s}_i + \mathbf{t} - \mathbf{s}_{i'})]_{\times} \mathbf{Q}_{i'}^T \mathbf{R} \mathbf{Q}_i \\ &= \mathbf{Q}_{i'}^T [\mathbf{R} \mathbf{s}_i + \mathbf{t} - \mathbf{s}_{i'}]_{\times} \mathbf{R} \mathbf{Q}_i \\ &= \mathbf{Q}_{i'}^T (\mathbf{R} [\mathbf{s}_i]_{\times} + [\mathbf{t} - \mathbf{s}_{i'}]_{\times} \mathbf{R}) \mathbf{Q}_i. \end{aligned} \quad (7)$$

To derive the second and third equalities, a property that $[\mathbf{R} \mathbf{t}]_{\times} \mathbf{R} = \mathbf{R} [\mathbf{t}]_{\times}$, $\forall \mathbf{R} \in \text{SO}(3)$ is exploited. This formula changes \mathbf{E}_k from being quadratic in \mathbf{R} to linear in \mathbf{R} . It can be seen that Eqs. (4a) and (4b) is bilinear in the unknown \mathbf{R} and \mathbf{t} . Notably, these two equations are homogeneous in \mathbf{R} and are not homogeneous in \mathbf{t} . This inhomogeneity is the key that the scale of \mathbf{t} can be recovered. In Section 3.5, it shows that there are degenerate cases when the inhomogeneity disappears.

3.3 Minimal Configurations

For a single camera, it is demonstrated that two ACs are sufficient to recover the relative pose [16]. Generally speaking, two ACs provide 6 independent constraints, and there are 5DOF in the relative pose of a single camera. Thus there is one excess constraint. We can ignore excess constraints during the solver generation procedure.

For multi-camera systems, the minimal configurations are complicated. Given n ACs across m views, we will figure out all of the minimal configurations. Assume that one AC is captured by m -views of a multi-camera system. In this case, there are two kinds of unknowns. First, there are 5 unknowns for each oriented point in 3D space corresponding to an AC, including 3 for point position and 2 for direction. Second, there are $6(m-1)$ unknowns for the pose of m views considering the world reference can only be determined up to a rigid motion. In summary, there are $5n + 6(m-1)$ unknowns. Each AC introduces $2m$ knowns for point position and $4(m-1)$ independent parameters for affine transformations. In summary, there are $2mn + 4(m-1)n$ knowns.

A configuration belongs to a minimal problem if and only if the number of unknowns equals the number of knowns. The results of excess constraint, i.e., the number of knowns minus the number of unknowns, are shown in

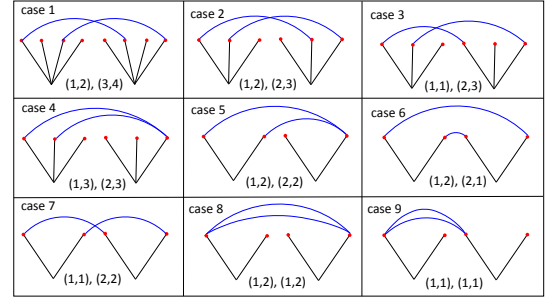


Fig. 3. Nine types of affine correspondence. Red dots represent perspective cameras; blue arcs represent affine correspondences. A pair (i, i') represents an AC that appears in the i -th camera in the first view and the i' -th camera in the second view.

Table 1. Zero indicates a minimal configuration. Positive numbers and negative numbers indicate over-determined and under-determined configurations, respectively. Since m and n are positive integers, $m = n = 2$ corresponds to the only minimal configuration. It should be mentioned that Table 1 summarizes the results for general settings. It is not necessarily held for special cases such as the relative pose has a motion prior, or the ACs are under partial visibility in multiple views.

There are many variants of minimal configurations. For example, 1AC+3PC across two views is also a minimal configuration. Another example is that one oriented point is captured by many perspective cameras in a view. It is redundant to enumerate all these variants. However, the solver generation procedure in this paper can be extended to these configurations in a straightforward way.

3.4 Categories of Two ACs Across Two Views

In the previous analysis, we draw a conclusion that two ACs across two views is a minimal configuration for a multi-camera system. By excluding one symmetry between individual perspective cameras and one symmetry between the two views, this configuration can be further classified into 9 cases, see Fig. 3. In the following, the AC type (i, i') means the AC appears in the i -th camera in the first view and the i' -th camera in the second view.

Among the 9 cases, the most common ones in practice are cases 6 and 7 for two-camera rigs. As shown in Fig. 3, case 6 uses inter-camera ACs, which is suitable for two-camera rigs with extensive overlapping of views. Case 7 uses intra-camera ACs, which is suitable for two-camera rigs with non-overlapping or small-overlapping of views. Cases 4 and 5 are useful for the incremental structure-from-motion based on a novel structure-less camera resection [54], [55], in which the collection of already reconstructed cameras are viewed as a generalized camera. Cases 8 and 9 are degenerate since they can be viewed as that two ACs are captured by a single perspective camera from two views.

3.5 Degenerate Cases

For multi-camera systems, the scale is observable due to \mathbf{E} is inhomogeneous in translation \mathbf{t} . In some special configurations, \mathbf{E} becomes homogeneous in translation \mathbf{t} , which

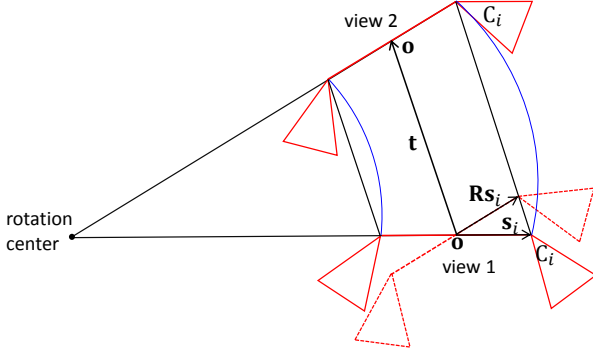


Fig. 4. A degenerate case due to constant rotation rate for case 7.

makes the scale unobservable. We prove three degenerate cases for multi-camera systems.

Proposition 1. *For case 6 in Fig. 3, when a multi-camera system undergoes pure translation and the translation direction is consistent with the baseline of two cameras, this configuration is degenerate. Specifically, the scale of translation cannot be recovered.*

Proof. Suppose the k -th AC appears in the i -th camera of view 1 and the i' -th camera of view 2. Since the translation direction is parallel with baseline of two camera, translation satisfies $\mathbf{s}_i - \mathbf{s}_{i'} = a\mathbf{t}$, where a is a unknown factor. In the case of pure translation, i.e., $\mathbf{R} = \mathbf{I}$, the essential matrix \mathbf{E}_k in Eq. (7) becomes

$$\begin{aligned}\mathbf{E}_k &= \mathbf{Q}_{i'}^T([\mathbf{t} + \mathbf{s}_i - \mathbf{s}_{i'}]_{\times})\mathbf{Q}_i \\ &= (a + 1)\mathbf{Q}_{i'}^T[\mathbf{t}]_{\times}\mathbf{Q}_i.\end{aligned}\quad (8)$$

The essential matrix is homogeneous with \mathbf{t} . For an arbitrary AC, the previous analysis holds. Thus the scale of translation cannot be recovered. \square

Proposition 2. *For case 7 in Fig. 3, the motion of pure translation or constant rotation rate is degenerate. Specifically, the scale of translation cannot be recovered.*

Proof. Suppose k -th AC appears in the i -th camera of view 1 and the i' -th camera of view 2. Since each AC is an intra-camera correspondence for case 7, we have $\mathbf{s}_i = \mathbf{s}_{i'}$ and $\mathbf{Q}_i = \mathbf{Q}_{i'}$.

For pure translation case, i.e., $\mathbf{R} = \mathbf{I}$, essential matrix in Eq. (7) becomes $\mathbf{E}_k = \mathbf{Q}_i^T[\mathbf{t}]_{\times}\mathbf{Q}_i$, which is homogeneous with \mathbf{t} . For the constant rotation rate case, the proof is inspired by [58] for PC-based solvers. In Fig. 4, both cameras move along with concentric circles. The two blue arcs are the camera trajectories moving along concentric circles. The motion of the multi-camera system is equivalent to a pure rotation \mathbf{R} at first, then proceed by a pure translation \mathbf{t} . The dotted multi-camera system is the result of view 1 under pure rotation. Point \mathbf{o} is the origin of the multi-camera system's reference. Without loss of generality, we assume that point \mathbf{o} lies on the two-camera rig's baseline. Take single camera C_i for an example, the pure rotation induced translation $\mathbf{R}\mathbf{s}_i - \mathbf{s}_i$ is aligned with the pure translation \mathbf{t} . Denote $\lambda\mathbf{t} = \mathbf{R}\mathbf{s}_i - \mathbf{s}_i$ and substitute it to Eq. (7), it can be verified that $\lambda\mathbf{t}$ invariably satisfies Eqs. (4a) and (4b). \square

Proposition 3. *Case 8 and case 9 in Fig. 3 are degenerate. Specifically, the translation cannot be recovered.*

Proof. These two cases can be viewed as that two ACs are captured by a single camera from two views. The relative rotation and translation can be recovered by a minimal solver for a single camera, such as [18] or the solver proposed in this paper. However, the recovered translation has scale-ambiguity for a single camera. The relative pose between a multi-camera system is a composition of three transformations, including two extrinsic parameters and the relative pose between two views of the single perspective camera. Due to the scale-ambiguity between two views of the perspective camera, the translation between two views of the multi-camera system cannot be recovered. \square

4 RELATIVE POSE RECOVERY FROM AFFINE CORRESPONDENCES

In this section, we propose a series of minimal solvers for all the cases in Fig. 3. The proposed solvers form a complete solution to relative pose estimation from ACs.

First of all, we need to parametrize the relative pose. Rotation can be parameterized by Cayley, quaternions, Euler angles, direction cosine matrix (DCM), etc. Cayley and quaternion parameterizations have shown superiority in minimal problems [26]. Rotation \mathbf{R} using Cayley parameterization can be written as

$$\mathbf{R}_{\text{cayl}} = \frac{1}{q_x^2 + q_y^2 + q_z^2 + 1} \cdot \begin{bmatrix} 1 + q_x^2 - q_y^2 - q_z^2 & 2q_xq_y - 2q_z & 2q_xq_z + 2q_y \\ 2q_xq_y + 2q_z & 1 - q_x^2 + q_y^2 - q_z^2 & 2q_yq_z - 2q_x \\ 2q_xq_z - 2q_y & 2q_yq_z + 2q_x & 1 - q_x^2 - q_y^2 + q_z^2 \end{bmatrix}, \quad (9)$$

where $[1, q_x, q_y, q_z]^T$ is a homogeneous quaternion vector. Note that 180-degree rotations are prohibited in Cayley parameterization, but this is a rare case for usual image pairs. In practice, it has been widely used in minimal problems [13], [26], [48], [54]. Rotation \mathbf{R} using quaternion parameterization can be written as

$$\mathbf{R}_{\text{quat}} = \begin{bmatrix} q_w^2 + q_x^2 - q_y^2 - q_z^2 & 2q_xq_y - 2q_wq_z & 2q_xq_z + 2q_wq_y \\ 2q_xq_y + 2q_wq_z & q_w^2 - q_x^2 + q_y^2 - q_z^2 & 2q_yq_z - 2q_wq_x \\ 2q_xq_z - 2q_wq_y & 2q_yq_z + 2q_wq_x & q_w^2 - q_x^2 - q_y^2 + q_z^2 \end{bmatrix}, \quad (10)$$

where $[q_w, q_x, q_y, q_z]^T$ is a normalized quaternion vector satisfying

$$q_w^2 + q_x^2 + q_y^2 + q_z^2 = 1. \quad (11)$$

In the following, we take Cayley parameterization as an example. The solver generation procedure can be applied to quaternion parameterization straightforwardly.

The translation \mathbf{t} can be written as

$$\mathbf{t} = [t_x \quad t_y \quad t_z]^T. \quad (12)$$

4.1 A Property of Rotation Matrices with Unknown Variables

A rotation matrix is an orthogonal matrix. We find a property for this kind of matrices, which is useful for relative pose estimation.

Theorem 1. Suppose a matrix $\mathbf{Q}_{3 \times 3}$ satisfies

$$\mathbf{Q}\mathbf{Q}^T = s^2\mathbf{I}, \quad s > 0, \quad (13)$$

where s is a polynomial of some variables. Suppose $\mathbf{a}_1^{(i)}, \mathbf{a}_2^{(i)}, \mathbf{a}_3^{(i)}, \mathbf{b}_1^{(i)}, \mathbf{b}_2^{(i)}, \mathbf{b}_3^{(i)} \in \mathbb{R}^3$ are arbitrary non-zero vectors. Then the polynomial of determinant

$$\mathbf{N} = \begin{bmatrix} \left(\sum_{i=1}^{m_1} \mathbf{a}_1^{(i)} \times \mathbf{Q}\mathbf{b}_1^{(i)} \right)^T \\ \left(\sum_{i=1}^{m_2} \mathbf{a}_2^{(i)} \times \mathbf{Q}\mathbf{b}_2^{(i)} \right)^T \\ \left(\sum_{i=1}^{m_3} \mathbf{a}_3^{(i)} \times \mathbf{Q}\mathbf{b}_3^{(i)} \right)^T \end{bmatrix} \quad (14)$$

has a factor s , where m_1, m_2, m_3 are positive integers.

The proof is provided in the supplementary material. \mathbf{R}_{quat} satisfies the condition (13) with $s = q_w^2 + q_x^2 + q_y^2 + q_z^2$. When an equation system is homogeneous in \mathbf{R}_{cayl} , we can safely omit the denominator in \mathbf{R}_{cayl} . It can be verified that the matrix $(1 + q_x^2 + q_y^2 + q_z^2)\mathbf{R}_{\text{cayl}}$ also satisfies the condition (13) with $s = 1 + q_x^2 + q_y^2 + q_z^2$. In the following, we will use this theorem to factor out s to simplify the equation system. It will generate more efficient solvers and sometimes avoid false roots.

In a few papers on relative pose estimation, a scale is factored out from the equation system for several specific parameterizations [26], [37]. The Theorem 1 provides a rigorous theory for a general form for the first time. We provide a good practice according to this theorem. For \mathbf{R}_{quat} , there is an equivalent form of Eq. (10): the diagonal elements can be replaced by $[1 - 2(q_y^2 + q_z^2), 1 - 2(q_x^2 + q_z^2), 1 - 2(q_x^2 + q_y^2)]^T$. This form does not satisfy the condition in Theorem 1. Thus the factor $(1 + q_x^2 + q_y^2 + q_z^2)$ cannot be factored out. It will usually cause a larger elimination template than using the form of Eq. (10). Using this practice, we obtain a new five-point solver for single cameras based on quaternion, which has a smaller elimination template than that proposed in [26].

4.2 Equation System Construction for Single Cameras

For the k -th affine correspondence, we obtain three polynomials for six unknowns $\{q_x, q_y, q_z, t_x, t_y, t_z\}$ from Eqs. (1) and (3) by substituting the essential matrix (2) into them. After separating q_x, q_y, q_z from t_x, t_y, t_z , we arrive at an equation system

$$\frac{1}{q_x^2 + q_y^2 + q_z^2 + 1} \underbrace{\overline{\mathbf{M}}_k(q_x, q_y, q_z)}_{3 \times 3} \begin{bmatrix} t_x \\ t_y \\ t_z \end{bmatrix} = \mathbf{0}, \quad (15)$$

where the entries of $\overline{\mathbf{M}}_k$ are quadratic polynomials with three unknowns q_x, q_y, q_z . Eq. (15) imposes three independent constraints on six unknowns $\{q_x, q_y, q_z, t_x, t_y, t_z\}$. Given two ACs, we get an equation system of 6 independent

constraints in a similar form as Eq. (15). By ignoring the scale factor, these equations are stacked by

$$\underbrace{\begin{bmatrix} \overline{\mathbf{M}}_1(q_x, q_y, q_z) \\ \overline{\mathbf{M}}_2(q_x, q_y, q_z) \end{bmatrix}}_{\overline{\mathbf{M}}_{6 \times 3}} \begin{bmatrix} t_x \\ t_y \\ t_z \end{bmatrix} = \mathbf{0}. \quad (16)$$

We use the hidden variable technique in equation system construction. The technique has been widely used in algebraic geometry for the elimination of variables from a multivariate polynomial system [59]. It can be seen that $\overline{\mathbf{M}}$ has a null vector. Its rank should be two for non-degenerate cases. (The rank cannot be less than two. Otherwise, the translation vector cannot be recovered.) Thus, the determinants of all the 3×3 submatrices of $\overline{\mathbf{M}}$ should be zero. There is a property for these submatrices.

Theorem 2. Suppose \mathbf{N} is an arbitrary 3×3 submatrix of $\overline{\mathbf{M}}$, the polynomial $\det(\mathbf{N})$ has a factor $q_x^2 + q_y^2 + q_z^2 + 1$.

The proof is based on Theorem 1, and it is provided in the supplementary material. Based on Theorem 2, the equation system is

$$\text{quot}(\det(\mathbf{N}), q_x^2 + q_y^2 + q_z^2 + 1) = 0, \quad \mathbf{N} \in 3 \times 3 \text{ submatrices of } \overline{\mathbf{M}}. \quad (17)$$

where $\text{quot}(a, b)$ means quotient of a divided by b , and $\det(\cdot)$ means the determinant operator.

There are two advantages to divide the determinants $\det(\mathbf{N})$ by $q_x^2 + q_y^2 + q_z^2 + 1$. First, the division eliminates the factor and avoids extraneous roots satisfying $q_x^2 + q_y^2 + q_z^2 + 1 = 0$. Though this equality cannot be satisfied in the real number field, it might be satisfied in the complex number field. Second, the order of the equation system can be reduced from 6 to 4.

There are 20 equations of degree 4 in Eq. (17). During solver generation, we ignore one excess constraint by removing the last row of $\overline{\mathbf{M}}$. Then there are 10 equations of degree 4. Once the rotation parameters $\{q_x, q_y, q_z\}$ have been obtained, the translation $[t_x, t_y, t_z]^T$ can be recovered by calculating the null space of $\overline{\mathbf{M}}$ up to a scale. The excess constraint is used to select the correct solution as that in [23].

4.3 Equation System Construction for Multi-Camera Systems

For the k -th affine correspondence, we obtain three polynomials for six unknowns $\{q_x, q_y, q_z, t_x, t_y, t_z\}$ from Eqs. (4a) and (4b) by substituting the essential matrix (7) into them. After separating q_x, q_y, q_z from t_x, t_y, t_z , we arrive at an equation system

$$\frac{1}{q_x^2 + q_y^2 + q_z^2 + 1} \underbrace{\mathbf{M}_k(q_x, q_y, q_z)}_{3 \times 4} \begin{bmatrix} t_x \\ t_y \\ t_z \\ 1 \end{bmatrix} = \mathbf{0}, \quad (18)$$

where the entries of \mathbf{M}_k are quadratic polynomials with three unknowns q_x, q_y, q_z .

Eq. (18) imposes three independent constraints on six unknowns $\{q_x, q_y, q_z, t_x, t_y, t_z\}$. Given two ACs, we get an equation system of 6 independent constraints in a similar

form as Eq. (18). By ignoring the scale factor, these equations are stacked by

$$\underbrace{\begin{bmatrix} \mathbf{M}_1(q_x, q_y, q_z) \\ \mathbf{M}_2(q_x, q_y, q_z) \end{bmatrix}}_{\mathbf{M}_{6 \times 4}} \begin{bmatrix} t_x \\ t_y \\ t_z \\ 1 \end{bmatrix} = \mathbf{0}. \quad (19)$$

It can be seen that \mathbf{M} has a null vector. Its rank should be three for non-degenerate cases. (The rank cannot be less than three. Otherwise, the translation vector cannot be recovered.) Thus, the determinants of all the 4×4 submatrices of \mathbf{M} should be zero. In addition, there is additional implicit constraints in this case. In the following, we prove that the rank of $(\mathbf{M}_k)_{(1:3,1:3)}$, $\forall k \in \{1, 2\}$ is 2.

Theorem 3. For non-degenerate cases, $\text{rank}(\mathbf{N}_k) = 2$, $\forall k$, where $\mathbf{N}_k = (\mathbf{M}_k)_{(1:3,1:3)}$.

Proof. Suppose the k -th AC appears in the i -th camera of view 1 and the i' -th camera of view 2.

First we prove that $\text{rank}(\mathbf{N}_k) \leq 2$. To achieve this goal, we need to prove that the null space of \mathbf{N}_k is not empty. According to Eq. (7), essential matrix \mathbf{E}_k is

$$\mathbf{E}_k = \mathbf{Q}_{i'}^T [\mathbf{t} + \mathbf{R}\mathbf{s}_i - \mathbf{s}_{i'}]_{\times} \mathbf{R}\mathbf{Q}_i. \quad (20)$$

Denote

$$\bar{\mathbf{t}} \triangleq \mathbf{t} + \mathbf{R}\mathbf{s}_i - \mathbf{s}_{i'}, \quad (21)$$

then we have

$$\mathbf{E}_k = \mathbf{Q}_{i'}^T [\bar{\mathbf{t}}]_{\times} \mathbf{R}\mathbf{Q}_i. \quad (22)$$

Substituting Eq. (22) into Eqs. (4a) and (4b), we obtain three equations. Each monomial in these three equations is linear with one entry of vector $\bar{\mathbf{t}}$, and there is no constant term. Thus these three equations can be formulated as

$$\frac{1}{q_x^2 + q_y^2 + q_z^2 + 1} \mathbf{A}_k \bar{\mathbf{t}} = \mathbf{0}, \quad (23)$$

$$\Rightarrow \mathbf{A}_k (\mathbf{t} + \mathbf{R}\mathbf{s}_i - \mathbf{s}_{i'}) = \mathbf{0}, \quad (24)$$

$$\Rightarrow [\mathbf{A}_k \quad \mathbf{A}_k(\mathbf{R}\mathbf{s}_i - \mathbf{s}_{i'})] \begin{bmatrix} \mathbf{t} \\ 1 \end{bmatrix} = \mathbf{0}. \quad (25)$$

By comparing the construction procedure of Eq. (18) and Eq. (25), we can see that

$$\mathbf{A}_k = (\mathbf{M}_k)_{(1:3,1:3)} = \mathbf{N}_k. \quad (26)$$

Substituting this equation into Eq. (23), we can see that the null space of \mathbf{N}_k is not empty.

Next we prove that $\text{rank}(\mathbf{N}_k) \geq 2$. We achieve this goal using proof by contradiction. If $\text{rank}(\mathbf{N}_k) \leq 1$, then $\text{rank}(\mathbf{M}_k) \leq 2$ considering that \mathbf{M}_k has one more column than \mathbf{N}_k . This means the k -th AC provides at most two independent constraints for the relative pose. This cannot be true for non-degenerate cases, so the assumption that $\text{rank}(\mathbf{N}_k) \leq 1$ is wrong. \square

Similar to the single camera case, there is also a property for some submatrices of \mathbf{M} .

Theorem 4. Suppose \mathbf{N} is an arbitrary 4×4 submatrix of \mathbf{M} or an arbitrary 3×3 submatrix of the first three columns of \mathbf{M} , the polynomial $\det(\mathbf{N})$ has a factor $q_x^2 + q_y^2 + q_z^2 + 1$.

The proof is based on Theorem 1, and it is provided in the supplementary material. Based on Proposition 4, we divide the determinants by factor $q_x^2 + q_y^2 + q_z^2 + 1$, and the constraints become

$$\mathcal{E}_1 \triangleq \{\text{quot}(\det(\mathbf{N}), q_x^2 + q_y^2 + q_z^2 + 1) = 0 \mid \mathbf{N} \in 4 \times 4 \text{ submatrices of } \mathbf{M}\}. \quad (27)$$

and

$$\mathcal{E}_2 \triangleq \{\text{quot}(\det(\mathbf{N}), q_x^2 + q_y^2 + q_z^2 + 1) = 0 \mid \mathbf{N} \in \{(\mathbf{M}_k)_{(1:3,1:3)}\}_{k=1,2}\} \quad (28)$$

There are 15 equations of degree 6 and two equations of degree 4 in \mathcal{E}_1 and \mathcal{E}_2 , respectively.

Once the rotation parameters $\{q_x, q_y, q_z\}$ have been obtained, the translation $[t_x, t_y, t_z]^T$ can be recovered by first calculating a vector in the null space of \mathbf{M} , and then normalizing the vector by dividing its last entry.

Remark: We provide an explanation to Proposition 3. Vector $\bar{\mathbf{t}}$ is the translation vector between the i -th camera in view 1 and the i' -th camera in view 2, which is expressed in view 1. If an AC is captured by a single camera, the equation system is homogeneous in \mathbf{t} . In contrast, if an AC is captured by a multi-camera system, the equation system is inhomogeneous in \mathbf{t} . When an AC is captured by a multi-camera system, it still satisfies the two-view geometry for a single camera by using proper translation.

4.4 Instantiation in A Finite Prime Field

Equation system (17) and equation system (27)(28) can be solved by Gröbner basis method [60], which is a general method to solve polynomial equation systems. Automatic solver generators [61], [62] can be used to construct solvers based on the Gröbner basis method. The most critical and challenging step in automatic solver generation is constructing a random instance of the original equation system in a finite prime field \mathbb{Z}_p [63]. This step aims to keep numerical stability and avoid large number arithmetic during the calculation of Gröbner basis. When constructing the random instance, the relations between the coefficients should be appropriately preserved. Otherwise, setting random values of the equation coefficients would destroy the latent relations and might result in a different problem without any solution. The technique of instantiation has been used in many minimal problems [11], [26], [64], [65].

In our problem, the coefficients of the equation systems are not fully independent since they are determined by certain latent relations. During the instantiation of our problem, we take advantage of basic operations in previous literature [64] and develop new operations in a finite field. In our problem, some new operations in \mathbb{Z}_p should be defined. First, random oriented points (or infinitesimal patches equivalently) in 3D space should be defined appropriately. Each patch is defined by a point \mathbf{p} and a unit normal \mathbf{n} in 3D space. The equation of the plane is $\mathbf{n}^T(\mathbf{y} - \mathbf{p}) = 0$, where \mathbf{y} is an arbitrary point in the plane. Since there is no square root for each number in finite prime fields, we need to try several times to generate a random unit normal. Second, the signed distance d_0 from a point \mathbf{y}_0 to previously defined plane is calculated by $d_0 = \mathbf{n}^T(\mathbf{y}_0 - \mathbf{p})$ in \mathbb{Z}_p . Third,

TABLE 2

Minimal solvers for 6DOF relative pose estimation of multi-camera systems. cayl: Cayley; quat: quaternion; inter: inter-camera correspondence (case 6); intra: intra-camera correspondence (case 7).

configuration	equations \mathcal{E}_1			equations $\mathcal{E}_1 + \mathcal{E}_2$		
	#sym	#sol	template	#sym	#sol	template
2ac+cayl+(case 1-5)	0	64	99×163	0	48	72×120
2ac+cayl+inter(case 6)	0	56	56×120	0	48	64×120
2ac+cayl+intra(case 7)	0	1-dim	—	0	48	72×120
2ac+quat+(case 1-5)	1	128	342×406	1	96	152×200
2ac+quat+inter(case 6)	1	112	178×243	1	96	152×200
2ac+quat+intra(case 7)	1	1-dim	—	1	96	152×200

when a plane is captured by two views of a single camera, the homography is calculated by $\mathbf{H} = \mathbf{R}' + \frac{1}{d}\mathbf{t}'\mathbf{n}^T$, where $[\mathbf{R}', \mathbf{t}']$ is the relative pose from the first view to the second view, \mathbf{n} is the unit normal of the plane expressed in the first view, and d is the signed distance from the optical center of the first view to the plane. Finally, the affine transformation \mathbf{A} can be calculated given the homography \mathbf{H} and image coordinates of the point correspondence. The formula in the real number field can be found in [18]. Since there is only addition, subtraction, multiplication, and division in this formula, it can be directly transferred to finite prime field \mathbb{Z}_p using the same form.

4.5 A Series of Solvers

The solver generator of Larsson et al. [62] was used to find a series of solvers for different cases. `Macaulay 2` [66] is used to calculate Gröbner basis. Both the Cayley and quaternion parameterizations are exploited.

For a single camera and Cayley parameterization, the solver has 20 solutions, and the elimination template is 36×56 . For quaternion parameterization, the solver has 40 solutions with one symmetry, and the elimination template is 60×80 .

For a multi-camera system, the statistics of the resulted solvers are shown in Table 2. #sym represents the number of symmetries, and #sol represents the number of solutions. 1-dim represents one dimensional extraneous roots. We have the following observations. (1) Cases 1 ~ 5 have the same solver. These cases can be viewed as one category. (2) If only \mathcal{E}_1 is used, cases 1 ~ 5 maximally have 64 complex solutions. Case 6 has 56 complex solutions. However, case 7 has one-dimensional families of extraneous roots. (3) If both \mathcal{E}_1 and \mathcal{E}_2 are used, cases 1 ~ 7 have 48 complex solutions. (4) Using equations from $\mathcal{E}_1 + \mathcal{E}_2$ results in smaller eliminate templates than using \mathcal{E}_1 only; using Cayley parameterization results in smaller eliminate templates than using quaternion parameterization. So the Cayley parameterization is preferred. (5) For quaternion parameterization, we also tested the method without factoring out the factor $q_x^2 + q_y^2 + q_z^2 + q_w^2$. It results in larger eliminate templates, demonstrating the effectiveness of factoring out the factor.

As shown in Proposition 3, cases 8 and 9 are degenerate. In these two cases, the rotation can be uniquely recovered, but the translation cannot be recovered. The proof of Proposition 3 provides a method of recovering the rotation. The core component is the relative pose for a single camera. We use our minimal solver to estimate the relative pose of a single camera.

At first glance, using solvers resulted from equations $\mathcal{E}_1 + \mathcal{E}_2$ is the first choice since they have a small number of solutions than using \mathcal{E}_1 only. However, we found that solvers from \mathcal{E}_1 have better numerical stability for case 6. The phenomenon that a larger number of basis than minimal requirement might have better numerical stability has been observed in previous literature [67], [68]. An empirical comparison of numerical stability is shown in the experiments.

5 RELATIVE POSE RECOVERY FROM POINT CORRESPONDENCES

In [11], a seminal six-point method is proposed for estimating the relative pose of generalized cameras. In this method, a generalized camera is formed by abstracting landmark observations into spatial rays. In practice, the most common generalized camera is the multi-camera system. We propose a new six-point method for multi-camera systems. Our method is based on the same framework for generating AC-based solvers, demonstrating its versatility.

5.1 Equation System Construction and Solving

For the relative pose estimation from PCs, the equation system construction and solving is essentially the same as the case of AC in Sections 3 and 4. One PC in a multi-camera system relates two perspective cameras across two views. Denote the k -th PC as $(\mathbf{x}_k, \mathbf{x}'_k, i_k, i'_k)$. It represents that a point is captured by the i_k -th camera in the first view, and its homogeneous coordinate in the normalized image plane is \mathbf{x}_k . It is also captured by the i'_k -th camera in the second view, and its homogeneous coordinate is \mathbf{x}'_k . To simplify the notation, we omit the subscript k of camera indices i and i' in the following text. The equation introduced by the k -th PC is same as Eq. (4a), and the essential matrix \mathbf{E}_k is determined by Eq. (7). We re-write them as below

$$\mathbf{x}_k'^T \mathbf{E}_k \mathbf{x}_k = 0, \quad (29)$$

where

$$\mathbf{E}_k = \mathbf{Q}_{i'}^T (\mathbf{R}[\mathbf{s}_i]_{\times} + [\mathbf{t} - \mathbf{s}_{i'}]_{\times} \mathbf{R}) \mathbf{Q}_i. \quad (30)$$

It is well-known that 6PC is a minimal configuration for relative pose estimation of generalized cameras. Using Cayley parameterization, there are 6 equations of the form (29). By using Cayley parametrization, these equations can be reformulated as

$$\underbrace{\widehat{\mathbf{M}}(q_x, q_y, q_z)}_{6 \times 4} \begin{bmatrix} t_x \\ t_y \\ t_z \\ 1 \end{bmatrix} = \mathbf{0}, \quad (31)$$

where the entries of $\widehat{\mathbf{M}}$ are quadratic polynomials with three unknowns q_x, q_y, q_z . The i -th row corresponds to the constraint of i -th PC. It can be seen that $\widehat{\mathbf{M}}$ has a null vector. Thus, the determinants of all the 4×4 submatrices of $\widehat{\mathbf{M}}$ should be zero.

For a family of PCs which relates the same perspective cameras across two views, there is one property.

Theorem 5. For non-degenerate cases, $\text{rank}(\mathbf{N}) = 2, \forall \mathbf{N} \in \mathcal{S}$. By Matlab syntax, \mathcal{S} is a set whose elements satisfying $\mathbf{N} =$

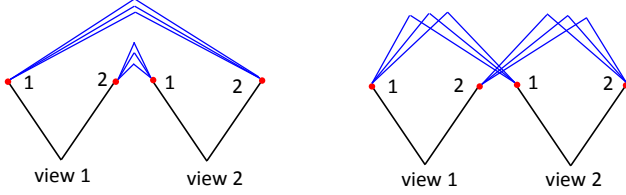


Fig. 5. Relative pose estimation from PCs for a multi-camera system. Six points are captured by two views of a two-camera rig. We aim to recover the 6DOF relative pose using 6 PCs. Left: inter-camera PCs; Right: intra-camera PCs.

TABLE 3

Minimal solvers for 6DOF relative pose estimation of multi-camera systems. cayl: Cayley; quat: quaternion; inter: inter-camera correspondence; intra: intra-camera correspondence.

configuration	equations $\hat{\mathcal{E}}_1$			equations $\hat{\mathcal{E}}_1 + \hat{\mathcal{E}}_2$		
	#sym	#sol	template	#sym	#sol	template
6pt+cayl+inter	0	56	56×120	0	48	64×120
6pt+cayl+intra	0	1-dim	—	0	48	72×120
6pt+quat+inter	1	112	174×243	1	96	152×200
6pt+quat+intra	1	1-dim	—	1	96	152×200

$\widehat{\mathbf{M}}([k_1, k_2, k_3], 1 : 3)$, where k_1 -th, k_2 -th, and k_3 -th PCs are captured by the same perspective cameras across two views and $k_1 < k_2 < k_3$.

The proof of is provided in the supplementary material. Again, a factor $q_x^2 + q_y^2 + q_z^2 + 1$ can be factored out by applying Theorem 1. In summary, the constraints are

$$\hat{\mathcal{E}}_1 \triangleq \{\text{quot}(\det(\mathbf{N}), q_x^2 + q_y^2 + q_z^2 + 1) = 0 \mid \mathbf{N} \in 4 \times 4 \text{ submatrices of } \widehat{\mathbf{M}}\}. \quad (32)$$

and

$$\hat{\mathcal{E}}_2 \triangleq \{\text{quot}(\det(\mathbf{N}), q_x^2 + q_y^2 + q_z^2 + 1) = 0 \mid \mathbf{N} \in \mathcal{S}\}. \quad (33)$$

There are 15 equations of degree 6 in $\hat{\mathcal{E}}_1$. The number of equations in $\hat{\mathcal{E}}_2$ varies for different PC configurations. $\hat{\mathcal{E}}_2$ might be empty set for certain configurations.

We consider 2 configurations for two-camera rigs. They are denoted as 6pt+inter and 6pt+intra, see Fig. 5. Both of them have two constraints in \mathcal{E}_2 . The statistics of the resulted solvers are shown in Table 3. For 6pt+quat+inter configuration, an inequality $q_w \neq 0$ should be explicitly considered when using $\hat{\mathcal{E}}_1$ only. Otherwise, there is one-dimensional extraneous roots. We consider this inequality by the saturation method [69], and obtain 112 solutions with one symmetry.

5.2 Relationship of AC-based and PC-based Solvers

When a plane is viewed in a pair of images, it is well-known that a homography relates the images of the plane [1]. This is held for perspective cameras. For affine cameras, the homography can be simplified as an affine transformation. The key requirement for an affinity is that the imaging rays in each view are parallel, i.e., an orthogonal projection occurs. For perspective cameras, the affinity cannot be strictly held for image regions. However, local affinity is still satisfied for infinite-small neighborhoods of a point

correspondence. An affine transformation is the first-order Taylor approximation of the related homography, i.e., it is tangent to the homography at the feature position [15], [70].

It was proved that one AC imposes three linear dependent constraints on relative pose [15], [16], [18], [19]. When constructing minimal configurations, 1AC can be roughly viewed as 3PCs. As a result, AC-based minimal solvers typically trisecting the number of minimum samples compared to PC-based counterparts. Take configurations 2ac+cayl+inter and 6pt+cayl+inter in this paper for an example, both of their minimal solvers have 48 solutions. When using the same solver generator [62], the sizes of their elimination templates are equal. Despite their close relationship, 1AC is not identical to 3 PCs [15].

There arises a question. Is it possible to hallucinate three PCs from one AC, and use PC-based solvers for AC observations? Since the affinity holds for infinite-small regions only, we cannot exactly hallucinate points even given a noise-free affinity. In addition, there is a trade-off during the hallucination. On the one hand, the inter-distance of the hallucinated points should be small enough such that the approximation error is not large. On the other hand, the inter-distance should be large enough to avoid numerical instability of near-degeneration. In practice, there are a few methods to hallucinate 3 PCs from 1 AC [71], [72]. It should be aware that hallucinated points will inevitably have approximation errors.

6 EXPERIMENTS

In this section, we conduct extensive experiments on synthetic and real-world data to evaluate the performance of the proposed solvers. For multi-camera systems, the proposed solvers are all based on Cayley parameterization. For AC-based solvers, we focus on inter-camera configuration (case 6) and intra-camera configuration (case 7). The solvers are referred to as 2AC-inter and 2AC-intra methods for inter-camera and intra-camera ACs, respectively. Sometimes we need to further distinguish two solvers for 2AC-inter. We use 2AC-inter-56 and 2AC-inter-48 to present solvers resulted from \mathcal{E}_1 and $\mathcal{E}_1 + \mathcal{E}_2$, respectively. For PC-based solvers, we focus on inter-camera and intra-camera configurations. Their solvers are referred to as 6pt-inter and 6pt-intra methods, respectively. Sometimes we need to further distinguish two solvers for 6pt-inter. We use 6pt-inter-56 and 6pt-inter-48 to present solvers resulted from $\hat{\mathcal{E}}_1$ and $\hat{\mathcal{E}}_1 + \hat{\mathcal{E}}_2$, respectively. The proposed solvers are compared with state-of-the-art solvers including 17pt-Li [12], 8pt-Kneip [13], and 6pt-Stewénus [11]. All the solvers are implemented in C++. The codes of comparison methods are provided by the OpenGV library [73].

In the real-world experiments, all the solvers are integrated into the RANSAC framework [4] to reject outliers. The relative pose which produces the largest number of inliers is chosen. By following the default parameters in OpenGV [73], the confidence of RANSAC is 0.99, and an inlier threshold angle is 0.1° . We demonstrate the feasibility of our methods on the KITTI dataset [3].

The rotation error is computed as the angular difference between the ground truth rotation and the estimated rotation: $\varepsilon_{\mathbf{R}} = \arccos((\text{trace}(\mathbf{R}_{\text{gt}}\mathbf{R}^T) - 1)/2)$, where \mathbf{R}_{gt} and

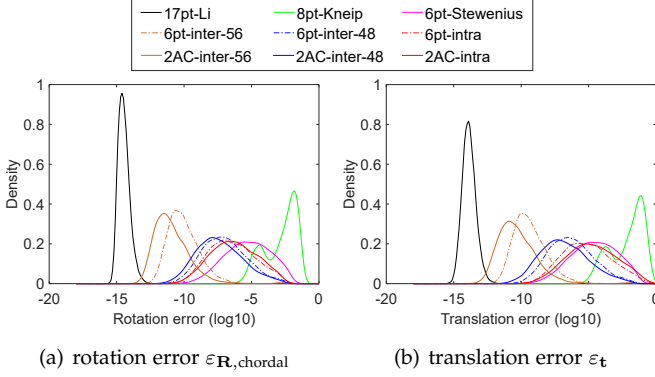


Fig. 6. Probability density functions over pose estimation errors on noise-free observations for multi-camera systems. The horizontal axis represents the \log_{10} errors, and the vertical axis represents the density.

\mathbf{R} are the ground truth and estimated rotation matrices, respectively. By following the definition in [36], [74], the translation error is defined as $\varepsilon_t = 2 \|\mathbf{t}_{gt} - \mathbf{t}\| / (\|\mathbf{t}_{gt}\| + \|\mathbf{t}\|)$, where \mathbf{t}_{gt} and \mathbf{t} are the ground truth and estimated translations. The translation direction error is defined by $\varepsilon_{t,dir} = \arccos(\mathbf{t}_{gt}^T \mathbf{t} / (\|\mathbf{t}_{gt}\| \cdot \|\mathbf{t}\|))$.

6.1 Efficiency and Numerical Stability

The runtimes of our solvers and the comparative solvers are evaluated using an Intel(R) Core(TM) i7-7800X 3.50GHz. Table 4 shows the average runtime of the solvers over 10,000 runs for multi-camera systems. The proposed solvers take 1.4 ~ 1.7 milliseconds. Among the minimal solvers, all the proposed solvers are more efficient than another minimal solver 6pt-Stewenius. Since 17pt-Li is a linear solver, it is the most efficient. As shown later, the proposed solvers need fewer correspondences than comparison methods and thus have better overall efficiency when integrating them into RANSAC.

Figure 6 reports the numerical stability of the solvers on noise-free observations¹. The procedure is repeated 10,000 times. The numerical error for rotation is measured by $\varepsilon_{\mathbf{R},choral} = \min_i \|\mathbf{R}_i - \mathbf{R}_{gt}\|$, where i counts all real solutions. The numerical error for translation is measure by ε_t . We did not use $\varepsilon_{\mathbf{R}}$ to evaluate numerical stability because the arccos function will introduce non-negligible numerical errors. The empirical probability density functions are plotted as the function of the \log_{10} estimated errors $\varepsilon_{\mathbf{R},choral}$ and ε_t .

Among the AC-based minimal solvers, the proposed 2AC-inter-56 solver has significantly better numerical stability than 2AC-inter-48 and 2AC-intra solvers. Based on this result, we recommend 2AC-inter-56 as the default solver for inter-camera ACs. It will be used for the following experiments, and we refer to it as 2AC-inter.

Among the PC-based minimal solvers, the proposed 6pt-inter-56 solver has significantly better numerical stability than 6pt-inter-48, 6pt-intra and 6pt-Stewenius solvers. Based on this result, we recommend 6pt-inter-56 as the default solver for inter-camera

1. For 2AC-intra and 6pt-intra, a technique is used to improve their numerical stability. More details can be found in the supplementary material.

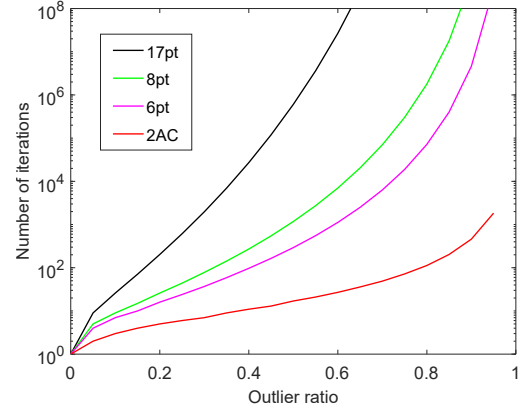


Fig. 7. RANSAC iteration number with respect to outlier ratio for success probability 0.99.

PCs. It will be used for the following experiments, and we refer to it as 6pt-inter. 17pt-Li has the best numerical stability since it is a linear solver and needs the fewest calculations. The 8pt-Kneip method based on iterative optimization is susceptible to falling into local minima and has the worst numerical stability.

In addition to efficiency and numerical stability, the minimal number of required geometric primitives is also an important factor for a solver. The iteration number N of RANSAC is determined by $N = \log(1-p) / \log(1-(1-\epsilon)^s)$, where s is the minimal number of required geometric primitives, ϵ is the outlier ratio, and p is the success probability. For a success probability 0.99, the RANSAC iterations needed with respect to the outlier ratio are shown in Fig.7. It can be seen that the iteration number of the RANSAC estimator increases exponentially with respect to the number s . For example, given a percentage of outliers $\epsilon = 50\%$, when the solvers require 17, 8, 6 and 2 primitives, the RANSAC needs 603607, 1177, 292 and 16 iterations, respectively. Since the proposed AC-based solvers need only two geometric primitives, they can be used efficiently for outlier detection when integrating them into the RANSAC framework. As we will see later, the proposed AC-based solvers have better overall efficiency than PC-based solvers.

6.2 Experiments on Synthetic Data

We defined a simulated forward-facing two-camera rig by following the KITTI autonomous driving platform [3]. The baseline length between the two simulated cameras is set to 1 meter. The multi-camera reference frame is defined at the middle of the camera rig, and the translation between two multi-camera reference frames is 3 meters. The resolution of the cameras is 640×480 pixels, and the focal lengths are 400 pixels. The principal points are set to the image center.

The synthetic scene is made up of a ground plane and 50 random planes, which are randomly generated in a cube of $[-5, 5] \times [-5, 5] \times [10, 20]$ meters, which are expressed in the respective axis of the multi-camera reference frame. We choose 50 ACs from the ground plane and an AC from each random plane randomly. Thus, there are 100 ACs generated randomly in the synthetic data. For each AC, a random 3D point from a plane is reprojected onto two cameras to get an image point pair. The associated affine transformation

TABLE 4
Runtime comparison of solvers for multi-camera systems (unit: μs).

method	17pt-Li [12]	8pt-Kneip [13]	6pt-Stewénius [11]	6pt-inter-56	6pt-inter-48	6pt-intra	2AC-inter-56	2AC-inter-48	2AC-intra
mean time	43.3	102.0	3275.4	1629.3	1416.4	1410.5	1669.5	1451.7	1491.8

is obtained by the following procedure. First, four points are chosen in view 1 that are vertices of a square, where the center of the square is the projected point of an AC. The side length of the square is set as 30 or 40 pixels. A larger side length causes smaller affinity noise. Second, the four corresponding points in view 2 are determined by the ground truth homography. Third, the sampled point pairs are contaminated by Gaussian noise. Fourth, we estimate a noisy homography using noisy point pairs. The noisy affine transformation is the first-order approximation of the noisy homography matrix.

A total of 1000 trials are carried out in the synthetic experiment. In each trial, 100 ACs are generated randomly. Two ACs for the proposed methods are selected randomly. The error is measured on the best relative pose, which produces the most inliers within the RANSAC scheme. The RANSAC scheme also allows us to select the best candidate from multiple solutions. The median of errors is used to assess the rotation and translation errors. In this set of experiments, the translation direction between two multi-camera references is chosen to produce either forward, sideways, or random motions. For each motion, the second view is perturbed by a random rotation. This random rotation is rotated around three axes in order, and the rotation angles range from -10° to 10° .

Figure 8 demonstrates the performance of different methods against image noise. Solid lines indicate using inter-camera correspondences, and dash-dotted lines indicate using intra-camera correspondences. We have the following observations. (1) Using inter-camera correspondences has better performance than using intra-camera correspondences. (2) The performance of AC-based methods is influenced by the magnitude of affinity noise, determined by the support region of sampled points. When the side length of the square is 40 pixels, the proposed 2AC-based methods have better or comparable performance than the comparative methods. (3) The proposed PC-based methods have better performance than 6pt-Stewénius. (4) The iterative optimization in 8pt-Kneip is susceptible to falling into local minima. It performs well for forward motion. However, it does not perform well for the other two motion modes, especially when using intra-cam PCs. Sometimes the error curves are out of the display range.

6.3 Experiments on Real-World Data

We test the performance of our methods on the KITTI dataset [3], which consists of successive video frames from a forward-facing stereo camera. The sequences labeled from 00 to 10 that have ground truth are used for the evaluation. Therefore, the methods were tested on a total of 23000 image pairs. The ACs between consecutive frames in each camera are established by applying the ASIFT [75]. It can also be obtained by MSER [76] which will be slightly less accurate

TABLE 5
Rotation and translation error of multi-camera systems on KITTI sequences (unit: degree).

Seq.	17pt-Li		8pt-Kneip		6pt-Stew		6pt-intra		2AC-intra	
	ϵ_R	$\epsilon_{t,dir}$	ϵ_R	$\epsilon_{t,dir}$	ϵ_R	$\epsilon_{t,dir}$	ϵ_R	$\epsilon_{t,dir}$	ϵ_R	$\epsilon_{t,dir}$
00	0.139	2.412	0.130	2.400	0.229	4.007	0.168	3.311	0.123	2.291
01	0.158	5.231	0.171	4.102	0.762	41.19	0.335	16.24	0.139	2.863
02	0.123	1.740	0.126	1.739	0.186	2.508	0.152	2.294	0.118	1.658
03	0.115	2.744	0.108	2.805	0.265	6.191	0.158	4.073	0.104	2.506
04	0.099	1.560	0.116	1.746	0.202	3.619	0.173	2.887	0.093	1.615
05	0.119	2.289	0.112	2.281	0.199	4.155	0.141	2.964	0.107	2.216
06	0.116	2.071	0.118	1.862	0.168	2.739	0.152	2.427	0.110	1.814
07	0.119	3.002	0.112	3.029	0.245	6.397	0.171	4.045	0.126	2.715
08	0.116	2.386	0.111	2.349	0.196	3.909	0.151	3.135	0.091	2.267
09	0.133	1.977	0.125	1.806	0.179	2.592	0.157	2.552	0.119	1.723
10	0.127	1.889	0.115	1.893	0.201	2.781	0.185	2.433	0.182	1.668

TABLE 6
Runtime of RANSAC averaged over KITTI sequences combined with different solvers (unit: second).

method	17pt-Li	8pt-Kneip	6pt-Stew	6pt-intra	2AC-intra
mean time	52.82	10.36	79.76	48.93	5.15
std. deviation	2.62	1.59	4.52	3.17	0.38

but much faster to obtain [77]. We ignore the overlap in their fields of view and treat it as a general multi-camera system. The ACs across the two cameras are not matched, and the translation scale is not estimated as the movement between consecutive frames is small. Instead, integrating the acceleration over time from an IMU is more suitable for recovering the translation scale [78]. All the solvers have been integrated into a RANSAC scheme to deal with outliers.

The proposed 2AC-intra and 6pt-intra methods are compared with 17pt-Li [12], 8pt-Kneip [13], and 6pt-Stewénius [11]. The results of the rotation and translation estimation are shown in Table 5. The 2AC-intra offers the best overall performance among all the methods. The 6pt-intra has consistently better performance than 6pt-Stewénius. In Fig. 9, the empirical cumulative distribution functions for KITTI sequence 00 are shown. It also demonstrates the proposed 2AC-intra offers the best overall performance in comparison to state-of-the-art methods.

The runtimes of RANSAC averaged over KITTI sequences combined with different solvers are shown in Table 6. Due to the benefits of computational efficiency, the 2AC-intra method is suitable for finding a correct inlier set, which is then used for accurate motion estimation in visual odometry.

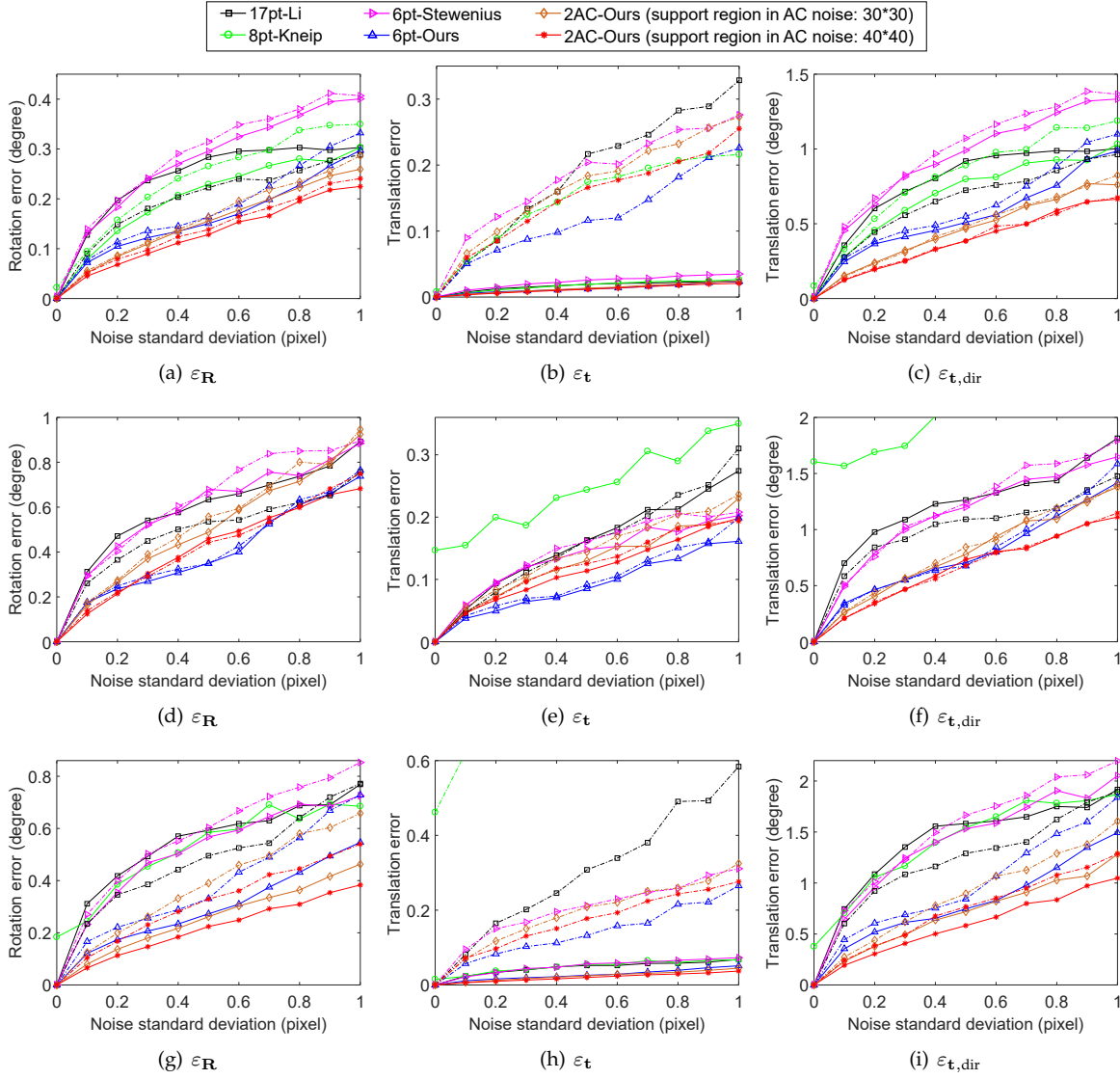


Fig. 8. Rotation and translation error with varying image noise. The first, second, and third rows correspond to forward, sideways, and random motions, respectively. Solid lines indicate using inter-camera ACs, and dash-dotted lines indicate using intra-camera ACs.

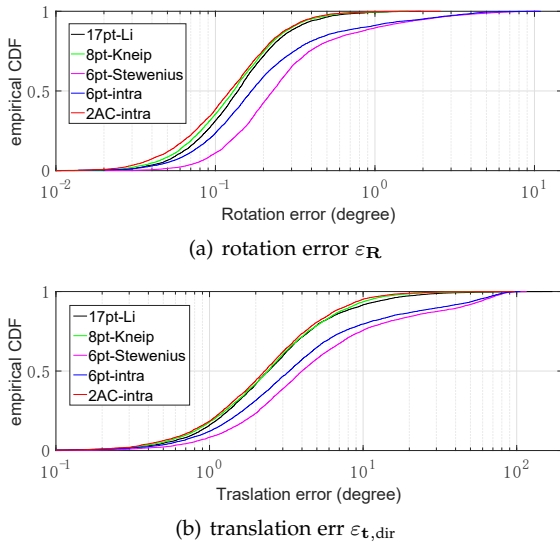


Fig. 9. Empirical cumulative distribution functions for KITTI sequence 00.

7 CONCLUSION

We proposed a complete solution and a series of solvers for relative pose estimation by exploiting affine correspondences. A minimum of two affine correspondences is used to estimate 6DOF relative pose of a multi-camera system. Two minimal solvers using point correspondences are also proposed for two-camera rigs. A few extensions to relative pose estimation with known rotation axis and/or unknown focal lengths are also proposed. All the proposed solvers are based on a unified and versatile framework. We evaluate the proposed solvers on both synthetic data and real-world image datasets. The experimental results demonstrated that the proposed solvers for multi-camera systems provide better overall efficiency and accuracy than state-of-the-art methods.

ACKNOWLEDGMENTS

The authors thank Dr. Qi Xie at Xi'an Jiaotong University for his help regarding the proofs.

REFERENCES

- [1] R. Hartley and A. Zisserman, *Multiple view geometry in computer vision*. Cambridge University Press, 2003.
- [2] R. Pless, "Using many cameras as one," in *IEEE Conference on Computer Vision and Pattern Recognition*, 2003, pp. 1–7.
- [3] A. Geiger, P. Lenz, C. Stiller, and R. Urtasun, "Vision meets robotics: The KITTI dataset," *The International Journal of Robotics Research*, vol. 32, no. 11, pp. 1231–1237, 2013.
- [4] M. A. Fischler and R. C. Bolles, "Random sample consensus: A paradigm for model fitting with applications to image analysis and automated cartography," *Communications of the ACM*, vol. 24, no. 6, pp. 381–395, 1981.
- [5] D. Nistér, "An efficient solution to the five-point relative pose problem," *IEEE Transactions on Pattern Analysis and Machine Intelligence*, vol. 26, no. 6, pp. 756–777, 2004.
- [6] H. Stewénius, C. Engels, and D. Nistér, "Recent developments on direct relative orientation," *ISPRS Journal of Photogrammetry and Remote Sensing*, vol. 60, no. 4, pp. 284–294, 2006.
- [7] H. Li and R. Hartley, "Five-point motion estimation made easy," in *International Conference on Pattern Recognition*, 2006, pp. 630–633.
- [8] L. Kneip, R. Siegwart, and M. Pollefeys, "Finding the exact rotation between two images independently of the translation," in *European Conference on Computer Vision*. Springer, 2012, pp. 696–709.
- [9] Z. Kukelova, M. Bujnak, and T. Pajdla, "Polynomial eigenvalue solutions to minimal problems in computer vision," *IEEE Transactions on Pattern Analysis and Machine Intelligence*, vol. 34, no. 7, pp. 1381–1393, 2012.
- [10] K. Fathian, J. P. Ramirez-Paredes, E. A. Doucette, J. W. Curtis, and N. R. Gans, "QuEst: A quaternion-based approach for camera motion estimation from minimal feature points," *IEEE Robotics and Automation Letters*, vol. 3, no. 2, pp. 857–864, 2018.
- [11] H. Stewénius, M. Oskarsson, K. Aström, and D. Nistér, "Solutions to minimal generalized relative pose problems," in *Workshop on Omnidirectional Vision in conjunction with ICCV*, 2005, pp. 1–8.
- [12] H. Li, R. Hartley, and J.-h. Kim, "A linear approach to motion estimation using generalized camera models," in *IEEE Conference on Computer Vision and Pattern Recognition*, 2008, pp. 1–8.
- [13] L. Kneip and H. Li, "Efficient computation of relative pose for multi-camera systems," in *IEEE Conference on Computer Vision and Pattern Recognition*, 2014, pp. 446–453.
- [14] J. Zhao, W. Xu, and L. Kneip, "A certifiably globally optimal solution to generalized essential matrix estimation," in *IEEE Conference on Computer Vision and Pattern Recognition*, 2020, pp. 12 034–12 043.
- [15] J. Bentolila and J. M. Francos, "Conic epipolar constraints from affine correspondences," *Computer Vision and Image Understanding*, vol. 122, pp. 105–114, 2014.
- [16] C. Raposo and J. P. Barreto, "Theory and practice of structure-from-motion using affine correspondences," in *IEEE Conference on Computer Vision and Pattern Recognition*, 2016, pp. 5470–5478.
- [17] D. Barath, T. Toth, and L. Hajder, "A minimal solution for two-view focal-length estimation using two affine correspondences," in *IEEE Conference on Computer Vision and Pattern Recognition*, 2017, pp. 6003–6011.
- [18] D. Barath and L. Hajder, "Efficient recovery of essential matrix from two affine correspondences," *IEEE Transactions on Image Processing*, vol. 27, no. 11, pp. 5328–5337, 2018.
- [19] I. Eichhardt and D. Chetverikov, "Affine correspondences between central cameras for rapid relative pose estimation," in *European Conference on Computer Vision*, 2018, pp. 488–503.
- [20] D. Barath, M. Polic, W. Fäurster, T. Sattler, T. Pajdla, and Z. Kukelova, "Making affine correspondences work in camera geometry computation," in *European Conference on Computer Vision*, 2020, pp. 723–740.
- [21] B. Guan, J. Zhao, Z. Li, F. Sun, and F. Fraundorfer, "Minimal solutions for relative pose with a single affine correspondence," in *IEEE Conference on Computer Vision and Pattern Recognition*, 2020, pp. 1929–1938.
- [22] L. Hajder and D. Barath, "Relative planar motion for vehicle-mounted cameras from a single affine correspondence," in *IEEE International Conference on Robotics and Automation*, 2020, pp. 8651–8657.
- [23] B. Guan, J. Zhao, D. Barath, and F. Fraundorfer, "Relative pose estimation for multi-camera systems from affine correspondences," *arXiv:2007.10700*, 2020.
- [24] T. Duff, K. Kohn, A. Leykin, and T. Pajdla, "PLMP - point-line minimal problems in complete multi-view visibility," in *IEEE International Conference on Computer Vision*, 2019, pp. 1675–1684.
- [25] R. Fabbri, T. Duff, H. Fan, M. H. Regan, D. d. C. d. Pinho, E. Tsagaridas, C. W. Wampler, J. D. Hauenstein, P. J. Giblin, B. Kimia, A. Leykin, and T. Pajdla, "TRPLP - trifocal relative pose from lines at points," in *IEEE Conference on Computer Vision and Pattern Recognition*, 2020, pp. 12 073–12 083.
- [26] J. Zhao, L. Kneip, Y. He, and J. Ma, "Minimal case relative pose computation using ray-point-ray features," *IEEE Transactions on Pattern Analysis and Machine Intelligence*, vol. 42, no. 5, pp. 1176–1190, 2020.
- [27] D. Barath, "Five-point fundamental matrix estimation for uncalibrated cameras," in *IEEE Conference on Computer Vision and Pattern Recognition*, 2018, pp. 235–243.
- [28] —, "Recovering affine features from orientation-and scale-invariant ones," in *Asian Conference on Computer Vision*. Springer, 2018, pp. 266–281.
- [29] D. Barath and Z. Kukelova, "Homography from two orientation-and scale-covariant features," in *IEEE International Conference on Computer Vision*, 2019, pp. 1091–1099.
- [30] D. G. Lowe, "Distinctive image features from scale-invariant keypoints," *International Journal of Computer Vision*, vol. 60, no. 2, pp. 91–110, 2004.
- [31] L. Kneip and S. Lynen, "Direct optimization of frame-to-frame rotation," in *IEEE International Conference on Computer Vision*, 2013, pp. 2352–2359.
- [32] J. Zhao, "An efficient solution to non-minimal case essential matrix estimation," *IEEE Transactions on Pattern Analysis and Machine Intelligence*, 2020.
- [33] R. I. Hartley, "In defense of the eight-point algorithm," *IEEE Transactions on Pattern Analysis and Machine Intelligence*, vol. 19, no. 6, pp. 580–593, 1997.
- [34] D. Barath and L. Hajder, "A theory of point-wise homography estimation," *Pattern Recognition Letters*, vol. 94, pp. 7–14, 2017.
- [35] O. Naroditsky, X. S. Zhou, J. Gallier, S. I. Roumeliotis, and K. Daniilidis, "Two efficient solutions for visual odometry using directional correspondence," *IEEE Transactions on Pattern Analysis and Machine Intelligence*, vol. 34, no. 4, pp. 818–824, 2012.
- [36] G. H. Lee, M. Pollefeys, and F. Fraundorfer, "Relative pose estimation for a multi-camera system with known vertical direction," in *IEEE Conference on Computer Vision and Pattern Recognition*, 2014, pp. 540–547.
- [37] C. Sweeney, J. Flynn, and M. Turk, "Solving for relative pose with a partially known rotation is a quadratic eigenvalue problem," in *International Conference on 3D Vision*, 2014, pp. 483–490.
- [38] O. Saurer, P. Vasseur, R. Bouteau, C. Démonceaux, M. Pollefeys, and F. Fraundorfer, "Homography based egomotion estimation with a common direction," *IEEE Transactions on Pattern Analysis and Machine Intelligence*, vol. 39, no. 2, pp. 327–341, 2016.
- [39] Y. Ding, J. Yang, J. Ponce, and H. Kong, "Homography-based minimal-case relative pose estimation with known gravity direction," *IEEE Transactions on Pattern Analysis and Machine Intelligence*, 2020.
- [40] M. V. Örnhaug, P. Persson, M. Wadenbäck, K. Aström, and A. Heyden, "Minimal solvers for indoor UAV positioning," *arXiv:2003.07111*, 2020.
- [41] B. Li, L. Heng, G. H. Lee, and M. Pollefeys, "A 4-point algorithm for relative pose estimation of a calibrated camera with a known relative rotation angle," in *IEEE/RSJ International Conference on Intelligent Robots and Systems*, 2013, pp. 1595–1601.
- [42] B. Li, E. Martyushev, and G. H. Lee, "Relative pose estimation of calibrated cameras with known SE(3) invariants," in *European Conference on Computer Vision*, 2020, pp. 215–231.
- [43] E. Martyushev and B. Li, "Efficient relative pose estimation for cameras and generalized cameras in case of known relative rotation angle," *Journal of Mathematical Imaging and Vision*, vol. 62, pp. 1076–1086, 2020.
- [44] S. Choi and J.-H. Kim, "Fast and reliable minimal relative pose estimation under planar motion," *Image and Vision Computing*, vol. 69, pp. 103–112, 2018.
- [45] D. Scaramuzza, "1-point-RANSAC structure from motion for vehicle-mounted cameras by exploiting non-holonomic constraints," *International Journal of Computer Vision*, vol. 95, no. 1, pp. 74–85, 2011.

- [46] G. H. Lee, F. Faundorfer, and M. Pollefeys, "Motion estimation for self-driving cars with a generalized camera," in *IEEE Conference on Computer Vision and Pattern Recognition*, 2013, pp. 2746–2753.
- [47] J. Ventura, C. Arth, and V. Lepetit, "An efficient minimal solution for multi-camera motion," in *IEEE International Conference on Computer Vision*, 2015, pp. 747–755.
- [48] H. Stewénius, D. Nistér, F. Kahl, and F. Schaffalitzky, "A minimal solution for relative pose with unknown focal length," in *IEEE Conference on Computer Vision and Pattern Recognition*, 2005, pp. 789–794.
- [49] R. Hartley and H. Li, "An efficient hidden variable approach to minimal-case camera motion estimation," *IEEE Transactions on Pattern Analysis and Machine Intelligence*, vol. 34, no. 12, pp. 2303–2314, 2012.
- [50] Z. Kukelova, J. Kileel, B. Sturm, and T. Pajdla, "A clever elimination strategy for efficient minimal solvers," in *IEEE Conference on Computer Vision and Pattern Recognition*, 2017, pp. 4912–4921.
- [51] Z. Kukelova and T. Pajdla, "A minimal solution to radial distortion autocalibration," *IEEE Transactions on Pattern Analysis and Machine Intelligence*, vol. 33, no. 12, pp. 2410–2422, 2011.
- [52] Y. Kuang, J. E. Solem, F. Kahl, and K. Aström, "Minimal solvers for relative pose with a single unknown radial distortion," in *IEEE Conference on Computer Vision and Pattern Recognition*, 2014, pp. 33–40.
- [53] I. Eichhardt and D. Barath, "Relative pose from deep learned depth and a single affine correspondence," in *European Conference on Computer Vision*, 2020, pp. 627–644.
- [54] E. Zheng and C. Wu, "Structure from motion using structure-less resection," in *IEEE International Conference on Computer Vision*, 2015, pp. 2075–2083.
- [55] Y. Kasten, M. Galun, and R. Basri, "Resultant based incremental recovery of camera pose from pairwise matches," in *IEEE Winter Conference on Applications of Computer Vision*, 2019, pp. 1080–1088.
- [56] L. Liu, H. Li, Y. Dai, and Q. Pan, "Robust and efficient relative pose with a multi-camera system for autonomous driving in highly dynamic environments," *IEEE Transactions on Intelligent Transportation Systems*, vol. 19, no. 8, pp. 2432–2444, 2017.
- [57] K. Alyousefi and J. Ventura, "Multi-camera motion estimation with affine correspondences," in *International Conference on Image Analysis and Recognition*, 2020, pp. 417–431.
- [58] B. Clipp, J.-H. Kim, J.-M. Frahm, M. Pollefeys, and R. Hartley, "Robust 6DOF motion estimation for non-overlapping, multi-camera systems," in *2008 IEEE Workshop on Applications of Computer Vision*. IEEE, 2008, pp. 1–8.
- [59] D. A. Cox, J. Little, and D. O'Shea, *Using algebraic geometry*. Springer Science & Business Media, 2006.
- [60] D. Cox, J. Little, and D. O'Shea, *Ideals, varieties, and algorithms: An introduction to computational algebraic geometry and commutative algebra*. Springer Science & Business Media, 2013.
- [61] Z. Kukelova, M. Bujnak, and T. Pajdla, "Automatic generator of minimal problem solvers," in *European Conference on Computer Vision*. Springer, 2008, pp. 302–315.
- [62] V. Larsson, K. Aström, and M. Oskarsson, "Efficient solvers for minimal problems by syzygy-based reduction," in *IEEE Conference on Computer Vision and Pattern Recognition*, 2017, pp. 820–828.
- [63] R. Lidl and H. Niederreiter, *Finite Fields*. Cambridge University Press, 1997.
- [64] M. Bujňák, "Algebraic solutions to absolute pose problems," Ph.D. dissertation, Department of Cybernetics, Czech Technical University in Prague, 2012.
- [65] J. B. Pritts, Z. Kukelova, V. Larsson, Y. Lochman, and O. Chum, "Minimal solvers for rectifying from radially-distorted conjugate translations," *IEEE Transactions on Pattern Analysis and Machine Intelligence*, 2020.
- [66] D. R. Grayson and M. E. Stillman, "Macaulay 2, a software system for research in algebraic geometry," <https://faculty.math.illinois.edu/Macaulay2/>, 2002.
- [67] M. Byröd, K. Josephson, and K. Aström, "Fast and stable polynomial equation solving and its application to computer vision," *International Journal of Computer Vision*, vol. 84, no. 3, pp. 237–256, 2009.
- [68] V. Larsson, M. Oskarsson, K. Aström, A. Wallis, Z. Kukelova, and T. Pajdla, "Beyond Gröbner bases: Basis selection for minimal solvers," in *IEEE Conference on Computer Vision and Pattern Recognition*, 2018, pp. 3945–3954.
- [69] V. Larsson, K. Aström, and M. Oskarsson, "Polynomial solvers for saturated ideals," in *IEEE International Conference on Computer Vision*, 2017, pp. 2288–2297.
- [70] K. Koser, C. Beder, and R. Koch, "Conjugate rotation: Parameterization and estimation from an affine feature correspondence," in *IEEE Conference on Computer Vision and Pattern Recognition*, 2008, pp. 1–8.
- [71] O. Chum, J. Matas, and Š. Obdržálek, "Epipolar geometry from three correspondences," in *Computer Vision Winter Workshop (CVWW'03)*, 2003.
- [72] F. Riggi, M. Toews, and T. Arbel, "Fundamental matrix estimation via TIP-transfer of invariant parameters," in *International Conference on Pattern Recognition*, vol. 2. IEEE, 2006, pp. 21–24.
- [73] L. Kneip and P. Furgale, "OpenGV: A unified and generalized approach to real-time calibrated geometric vision," in *IEEE International Conference on Robotics and Automation*, 2014, pp. 1–8.
- [74] L. Quan and Z. Lan, "Linear n-point camera pose determination," *IEEE Transactions on Pattern Analysis and Machine Intelligence*, vol. 21, no. 8, pp. 774–780, 1999.
- [75] J.-M. Morel and G. Yu, "ASIFT: A new framework for fully affine invariant image comparison," *SIAM Journal on Imaging Sciences*, vol. 2, no. 2, pp. 438–469, 2009.
- [76] J. Matas, O. Chum, M. Urban, and T. Pajdla, "Robust wide-baseline stereo from maximally stable extremal regions," *Image and Vision Computing*, vol. 22, no. 10, pp. 761–767, 2004.
- [77] D. Barath, J. Matas, and L. Hajder, "Accurate closed-form estimation of local affine transformations consistent with the epipolar geometry," in *British Machine Vision Conference*, 2016.
- [78] G. Nützi, S. Weiss, D. Scaramuzza, and R. Siegwart, "Fusion of IMU and vision for absolute scale estimation in monocular SLAM," *Journal of intelligent & robotic systems*, vol. 61, no. 1-4, pp. 287–299, 2011.

Supplementary Material

APPENDIX A PROOF

A.1 Proof of Theorem 1

In this section, we use “ \cdot ” to represent dot product.

Lemma 1. *Properties of cross product:*

$$(i) \mathbf{a} \cdot (\mathbf{b} \times \mathbf{c}) = \begin{vmatrix} a_1 & a_2 & a_3 \\ b_1 & b_2 & b_3 \\ c_1 & c_2 & c_3 \end{vmatrix} = \begin{vmatrix} a_1 & b_1 & c_1 \\ a_2 & b_2 & c_2 \\ a_3 & b_3 & c_3 \end{vmatrix}, \text{ where}$$

$$\mathbf{a} = [a_1, a_2, a_3]^T, \mathbf{b} = [b_1, b_2, b_3]^T, \mathbf{c} = [c_1, c_2, c_3]^T.$$

(ii) $\mathbf{a} \times (\mathbf{b} \times \mathbf{c}) = \mathbf{b}(\mathbf{a} \cdot \mathbf{c}) - \mathbf{c}(\mathbf{a} \cdot \mathbf{b})$. This is known as triple product expansion, or Lagrange's formula.

(iii) $\mathbf{a} \cdot (\mathbf{b} \times \mathbf{c}) = \mathbf{b} \cdot (\mathbf{c} \times \mathbf{a}) = \mathbf{c} \cdot (\mathbf{a} \times \mathbf{b})$. The scalar triple product is unchanged under a circular shift of its three operands $(\mathbf{a}, \mathbf{b}, \mathbf{c})$.

(iv) $\mathbf{a} \times (\mathbf{b} + \mathbf{c}) = (\mathbf{a} \times \mathbf{b}) + (\mathbf{a} \times \mathbf{c})$.

(v) $\mathbf{a} \times \mathbf{b} = [\mathbf{a}]_{\times} \mathbf{b} = -[\mathbf{b}]_{\times} \mathbf{a}$.

The above properties can be found in [https://en.wikipedia.org/wiki/Cross_product] and [https://en.wikipedia.org/wiki/Triple_product].

Lemma 2. *Suppose \mathbf{Q} is a matrix satisfying*

$$\mathbf{Q}\mathbf{Q}^T = s^2 \mathbf{I} = \begin{bmatrix} s^2 & 0 & 0 \\ 0 & s^2 & 0 \\ 0 & 0 & s^2 \end{bmatrix}, s > 0 \quad (34)$$

then

$$\mathbf{Q}_i \times \mathbf{Q}_j = \begin{cases} s I_k \mathbf{Q}_k & \text{if } i \neq j, \\ 0 & \text{if } i = j. \end{cases} \quad (35)$$

where \mathbf{I} is an identity matrix, \mathbf{Q}_i is the i -th row (or column) of \mathbf{Q} , $I_k = +1$ or -1 , and $k = \{1, 2, 3\} \setminus \{i, j\}$.

Proof. When $i \neq j$, the direction of \mathbf{Q}_k is perpendicular to both \mathbf{Q}_i and \mathbf{Q}_j according to Eq. (34). Thus the direction of $\mathbf{Q}_i \times \mathbf{Q}_j$ is $\mathbf{n} := \frac{I_k \mathbf{Q}_k}{\|\mathbf{Q}_k\|} = \frac{1}{s} I_k \mathbf{Q}_k$. According to the definition of cross product, $\mathbf{Q}_i \times \mathbf{Q}_j = \sin \langle \mathbf{Q}_i, \mathbf{Q}_j \rangle \cdot \|\mathbf{Q}_i\| \cdot \|\mathbf{Q}_j\| \cdot \mathbf{n} = \sin(\pi/2) \cdot s \cdot s \cdot \frac{1}{s} I_k \mathbf{Q}_k = s I_k \mathbf{Q}_k$. When $i = j$, we have $\mathbf{Q}_i \times \mathbf{Q}_j = \mathbf{Q}_i \times \mathbf{Q}_i = 0$. \square

Lemma 3. *Suppose matrix $\mathbf{Q}_{3 \times 3}$ satisfies*

$$\mathbf{Q}\mathbf{Q}^T = s^2 \mathbf{I}, s > 0 \quad (36)$$

where s is a polynomial of some variables. Suppose $\mathbf{a}_1, \mathbf{a}_2, \mathbf{a}_3, \mathbf{b}_1, \mathbf{b}_2$, and $\mathbf{b}_3 \in \mathbb{R}^3$ are arbitrary non-zero vectors. Then the determinant of

$$\mathbf{N} = \begin{bmatrix} (\mathbf{a}_1 \times \mathbf{Q}\mathbf{b}_1)^T \\ (\mathbf{a}_2 \times \mathbf{Q}\mathbf{b}_2)^T \\ (\mathbf{a}_3 \times \mathbf{Q}\mathbf{b}_3)^T \end{bmatrix} \quad (37)$$

has a factor s .

Proof. According to the properties of cross product in Lemma 1, we have

$$\begin{aligned} \det(\mathbf{N}) &= \det(\mathbf{N}^T) \\ &= \det([\mathbf{a}_1 \times \mathbf{Q}\mathbf{b}_1, \mathbf{a}_2 \times \mathbf{Q}\mathbf{b}_2, \mathbf{a}_3 \times \mathbf{Q}\mathbf{b}_3]) \\ &= (\mathbf{a}_1 \times \mathbf{Q}\mathbf{b}_1) \cdot [(\mathbf{a}_2 \times \mathbf{Q}\mathbf{b}_2) \times (\mathbf{a}_3 \times \mathbf{Q}\mathbf{b}_3)] \\ &= (\mathbf{a}_1 \times \mathbf{Q}\mathbf{b}_1) \cdot \\ &\quad \{ \mathbf{a}_3 [(\mathbf{a}_2 \times \mathbf{Q}\mathbf{b}_2) \cdot \mathbf{Q}\mathbf{b}_3] - \mathbf{Q}\mathbf{b}_3 [(\mathbf{a}_2 \times \mathbf{Q}\mathbf{b}_2) \cdot \mathbf{a}_3] \} \\ &= [(\mathbf{a}_1 \times \mathbf{Q}\mathbf{b}_1) \cdot \mathbf{a}_3] [(\mathbf{a}_2 \times \mathbf{Q}\mathbf{b}_2) \cdot \mathbf{Q}\mathbf{b}_3] \\ &\quad - [(\mathbf{a}_1 \times \mathbf{Q}\mathbf{b}_1) \cdot \mathbf{Q}\mathbf{b}_3] [(\mathbf{a}_2 \times \mathbf{Q}\mathbf{b}_2) \cdot \mathbf{a}_3] \\ &= [(\mathbf{a}_1 \times \mathbf{Q}\mathbf{b}_1) \cdot \mathbf{a}_3] [\mathbf{a}_2 \cdot (\mathbf{Q}\mathbf{b}_2 \times \mathbf{Q}\mathbf{b}_3)] \\ &\quad - [\mathbf{a}_1 \cdot (\mathbf{Q}\mathbf{b}_1 \times \mathbf{Q}\mathbf{b}_3)] [(\mathbf{a}_2 \times \mathbf{Q}\mathbf{b}_2) \cdot \mathbf{a}_3]. \end{aligned} \quad (38)$$

From the above equation, if all entries of $\mathbf{Q}\mathbf{b}_2 \times \mathbf{Q}\mathbf{b}_3$ and $\mathbf{Q}\mathbf{b}_1 \times \mathbf{Q}\mathbf{b}_3$ have a common factor s , the determinant $\det(\mathbf{N})$ should have the factor s too. In the following, we prove that all entries of $\mathbf{Q}\mathbf{a} \times \mathbf{Q}\mathbf{b}$ have the factor s for arbitrary vectors $\mathbf{a} = [a_1, a_2, a_3]^T$ and $\mathbf{b} = [b_1, b_2, b_3]^T$. Since \mathbf{Q} satisfies Eq. (34) in Lemma 2, we have

$$\begin{aligned} \mathbf{Q}\mathbf{a} \times \mathbf{Q}\mathbf{b} &= \left(\sum_{i=1}^3 a_i \mathbf{Q}_i \right) \times \left(\sum_{j=1}^3 b_j \mathbf{Q}_j \right) \\ &= \sum_{i=1}^3 \sum_{j \neq i} a_i b_j \mathbf{Q}_i \times \mathbf{Q}_j \\ &= \sum_{i=1}^3 \sum_{j \neq i, k \notin \{i, j\}} a_i b_j s I_k \mathbf{Q}_k \\ &= s [I_1 (a_2 b_3 - a_3 b_2) \mathbf{Q}_1 + I_2 (a_3 b_1 - a_1 b_3) \mathbf{Q}_2 \\ &\quad + I_3 (a_1 b_2 - a_2 b_1) \mathbf{Q}_3], \end{aligned} \quad (39)$$

where I_k equals $+1$ or -1 . It can be seen that s is a common factor for all entries in $\mathbf{Q}\mathbf{a} \times \mathbf{Q}\mathbf{b}$. \square

Theorem 1. *Suppose a matrix $\mathbf{Q}_{3 \times 3}$ satisfies*

$$\mathbf{Q}\mathbf{Q}^T = s^2 \mathbf{I}, s > 0 \quad (40)$$

where s is a polynomial of some variables. Suppose $\mathbf{a}_1^{(i)}, \mathbf{a}_2^{(i)}, \mathbf{a}_3^{(i)}, \mathbf{b}_1^{(i)}, \mathbf{b}_2^{(i)}$, and $\mathbf{b}_3^{(i)} \in \mathbb{R}^3$ are arbitrary non-zero vectors. Then the polynomial of determinant

$$\mathbf{N} = \begin{bmatrix} \left(\sum_{i=1}^{m_1} \mathbf{a}_1^{(i)} \times \mathbf{Q}\mathbf{b}_1^{(i)} \right)^T \\ \left(\sum_{i=1}^{m_2} \mathbf{a}_2^{(i)} \times \mathbf{Q}\mathbf{b}_2^{(i)} \right)^T \\ \left(\sum_{i=1}^{m_3} \mathbf{a}_3^{(i)} \times \mathbf{Q}\mathbf{b}_3^{(i)} \right)^T \end{bmatrix} \quad (41)$$

has a factor s , where m_1, m_2, m_3 are positive integers.

Proof. We prove this proposition for the case of $m_1 = m_2 = m_3 = 2$. The proof can be extended to other cases straightforwardly. Rewrite \mathbf{N} as the following form

$$\mathbf{N} = \begin{bmatrix} (\mathbf{a}_1 \times \mathbf{Q}\mathbf{b}_1 + \mathbf{c}_1 \times \mathbf{Q}\mathbf{d}_1)^T \\ (\mathbf{a}_2 \times \mathbf{Q}\mathbf{b}_2 + \mathbf{c}_2 \times \mathbf{Q}\mathbf{d}_2)^T \\ (\mathbf{a}_3 \times \mathbf{Q}\mathbf{b}_3 + \mathbf{c}_3 \times \mathbf{Q}\mathbf{d}_3)^T \end{bmatrix}. \quad (42)$$

Its determinant is

$$\begin{aligned}
& \det(\mathbf{N}) = \det(\mathbf{N}^T) \\
& = (\mathbf{a}_1 \times \mathbf{Qb}_1 + \mathbf{c}_1 \times \mathbf{Qd}_1) \cdot \\
& \quad [(\mathbf{a}_2 \times \mathbf{Qb}_2 + \mathbf{c}_2 \times \mathbf{Qd}_2) \times (\mathbf{a}_3 \times \mathbf{Qb}_3 + \mathbf{c}_3 \times \mathbf{Qd}_3)] \\
& = (\mathbf{a}_1 \times \mathbf{Qb}_1 + \mathbf{c}_1 \times \mathbf{Qd}_1) \cdot \\
& \quad [(\mathbf{a}_2 \times \mathbf{Qb}_2) \times (\mathbf{a}_3 \times \mathbf{Qb}_3) + (\mathbf{a}_2 \times \mathbf{Qb}_2) \times (\mathbf{c}_3 \times \mathbf{Qd}_3) \\
& \quad + (\mathbf{c}_2 \times \mathbf{Qd}_2) \times (\mathbf{a}_3 \times \mathbf{Qb}_3) + (\mathbf{c}_2 \times \mathbf{Qd}_2) \times (\mathbf{c}_3 \times \mathbf{Qd}_3)] \\
& = \det([\mathbf{a}_1 \times \mathbf{Qb}_1, \mathbf{a}_2 \times \mathbf{Qb}_2, \mathbf{a}_3 \times \mathbf{Qb}_3]) \\
& \quad + \det([\mathbf{a}_1 \times \mathbf{Qb}_1, \mathbf{a}_2 \times \mathbf{Qb}_2, \mathbf{c}_3 \times \mathbf{Qd}_3]) \\
& \quad + \det([\mathbf{a}_1 \times \mathbf{Qb}_1, \mathbf{c}_2 \times \mathbf{Qd}_2, \mathbf{a}_3 \times \mathbf{Qb}_3]) \\
& \quad + \det([\mathbf{a}_1 \times \mathbf{Qb}_1, \mathbf{c}_2 \times \mathbf{Qd}_2, \mathbf{c}_3 \times \mathbf{Qd}_3]) \\
& \quad + \det([\mathbf{c}_1 \times \mathbf{Qd}_1, \mathbf{a}_2 \times \mathbf{Qb}_2, \mathbf{a}_3 \times \mathbf{Qb}_3]) \\
& \quad + \det([\mathbf{c}_1 \times \mathbf{Qd}_1, \mathbf{a}_2 \times \mathbf{Qb}_2, \mathbf{c}_3 \times \mathbf{Qd}_3]) \\
& \quad + \det([\mathbf{c}_1 \times \mathbf{Qd}_1, \mathbf{c}_2 \times \mathbf{Qd}_2, \mathbf{a}_3 \times \mathbf{Qb}_3]) \\
& \quad + \det([\mathbf{c}_1 \times \mathbf{Qd}_1, \mathbf{c}_2 \times \mathbf{Qd}_2, \mathbf{c}_3 \times \mathbf{Qd}_3]). \tag{43}
\end{aligned}$$

According Lemma 3, each term in the right-hand side of Eq. (43) has a factor of s . Thus $\det(\mathbf{N})$ also has this factor. \square

A.2 Proof of Theorem 2

Lemma 4. Given an affine correspondence $(\mathbf{x}, \mathbf{x}', \mathbf{A})$ and essential matrix $\mathbf{E} = [\mathbf{t}]_{\times} \mathbf{R}$, the three constraints

$$\begin{aligned}
& \mathbf{x}'^T \mathbf{E} \mathbf{x} = 0 \tag{44a} \\
& (\mathbf{E}^T \mathbf{x}')_{(1:2)} + \mathbf{A}^T (\mathbf{E} \mathbf{x})_{(1:2)} = \mathbf{0} \tag{44b}
\end{aligned}$$

can be reformulated as

$$-\left[\begin{array}{c} (\mathbf{x}' \times \mathbf{R} \mathbf{x})^T \\ (\mathbf{x}' \times \mathbf{R} \mathbf{c}_1 + \mathbf{a}_1 \times \mathbf{R} \mathbf{x})^T \\ (\mathbf{x}' \times \mathbf{R} \mathbf{c}_2 + \mathbf{a}_2 \times \mathbf{R} \mathbf{x})^T \end{array} \right] \mathbf{t} = \mathbf{0}, \tag{45}$$

where $\mathbf{c}_1 = [1, 0, 0]^T$, $\mathbf{c}_2 = [0, 1, 0]^T$, $\mathbf{a}_1 = [\mathbf{A}_{11}, \mathbf{A}_{21}, 0]^T$, and $\mathbf{a}_2 = [\mathbf{A}_{12}, \mathbf{A}_{22}, 0]^T$.

Proof. For Eq. (44a), we have

$$\begin{aligned}
& \mathbf{x}'^T \mathbf{E} \mathbf{x} \\
& = \mathbf{x}'^T [\mathbf{t}]_{\times} \mathbf{R} \mathbf{x} = (\mathbf{R} \mathbf{x})^T (\mathbf{x}'^T [\mathbf{t}]_{\times})^T \\
& = -\mathbf{x}^T \mathbf{R}^T [\mathbf{t}]_{\times} \mathbf{x}' = \mathbf{x}^T \mathbf{R}^T [\mathbf{x}']_{\times} \mathbf{t} \\
& = (\mathbf{R} \mathbf{x} \times \mathbf{x}')^T \mathbf{t} = -(\mathbf{x}' \times \mathbf{R} \mathbf{x})^T \mathbf{t}. \tag{46}
\end{aligned}$$

For the first term of Eq. (44b), we have

$$\begin{aligned}
& \mathbf{E}^T \mathbf{x}' \\
& = ([\mathbf{t}]_{\times} \mathbf{R})^T \mathbf{x}' = -\mathbf{R}^T [\mathbf{t}]_{\times} \mathbf{x}' \\
& = \mathbf{I} \mathbf{R}^T [\mathbf{x}']_{\times} \mathbf{t}, \tag{47}
\end{aligned}$$

where \mathbf{I} is an identity matrix. In the above equation, the i -th entry of the right-hand side can be reformulated as

$$\mathbf{c}_i^T \mathbf{R}^T [\mathbf{x}']_{\times} \mathbf{t} = -(\mathbf{x}' \times \mathbf{R} \mathbf{c}_i)^T \mathbf{t}. \tag{48}$$

For the second term of Eq. (44b), its i -th ($i = 1, 2$) entry is $\mathbf{a}_i^T \mathbf{E} \mathbf{x}$. Similar to the derivation in Eq. (46), we have

$$\mathbf{a}_i^T \mathbf{E} \mathbf{x} = -(\mathbf{a}_i \times \mathbf{R} \mathbf{x})^T \mathbf{t}. \tag{49}$$

By combining Eq. (46), (48), and (49), the proof is completed. \square

Theorem 2. Suppose \mathbf{N} is an arbitrary 3×3 submatrix of $\overline{\mathbf{M}}$, the polynomial $\det(\mathbf{N})$ has a factor $q_x^2 + q_y^2 + q_z^2 + 1$.

Proof. Denote

$$\begin{aligned}
& \mathbf{Q} = (q_x^2 + q_y^2 + q_z^2 + 1) \mathbf{R} \\
& = \begin{bmatrix} 1 + q_x^2 - q_y^2 - q_z^2 & 2q_x q_y - 2q_z & 2q_y + 2q_x q_z \\ 2q_x q_y + 2q_z & 1 - q_x^2 + q_y^2 - q_z^2 & 2q_y q_z - 2q_x \\ 2q_x q_z - 2q_y & 2q_x + 2q_y q_z & 1 - q_x^2 - q_y^2 + q_z^2 \end{bmatrix}, \tag{50}
\end{aligned}$$

It can be verified that $\mathbf{Q} \mathbf{Q}^T = s^2 \mathbf{I}$ with $s = q_x^2 + q_y^2 + q_z^2 + 1$.

Recall that $\overline{\mathbf{M}}$ is composed of constraints from two affine correspondences, and \mathbf{N} is a 3×3 submatrix of $\overline{\mathbf{M}}$. According to Lemma 4, \mathbf{N} has the form of

$$\mathbf{N} = \begin{bmatrix} (\mathbf{a}_1 \times \mathbf{Qb}_1 + \mathbf{c}_1 \times \mathbf{Qd}_1)^T \\ (\mathbf{a}_2 \times \mathbf{Qb}_2 + \mathbf{c}_2 \times \mathbf{Qd}_2)^T \\ (\mathbf{a}_3 \times \mathbf{Qb}_3 + \mathbf{c}_3 \times \mathbf{Qd}_3)^T \end{bmatrix}. \tag{51}$$

Note that \mathbf{Q} instead of \mathbf{R} appears in this matrix because the scale factor $\frac{1}{q_x^2 + q_y^2 + q_z^2 + 1}$ is ignored during the equation system construction. Since all the conditions in Lemma 1 are satisfied, $\det(\mathbf{N})$ has a factor s . \square

A.3 Proof of Theorem 4

Lemma 5. For a multi camera system, denote the constraints introduced by the k -th affine correspondence as

$$\mathbf{x}_k'^T \mathbf{E}_k \mathbf{x}_k = 0 \tag{52a}$$

$$(\mathbf{E}_k^T \mathbf{x}_k')_{(1:2)} + \mathbf{A}_k^T (\mathbf{E}_k \mathbf{x}_k)_{(1:2)} = \mathbf{0} \tag{52b}$$

where

$$\mathbf{E}_k = \mathbf{Q}_i^T (\mathbf{R} [\mathbf{s}_i]_{\times} + [\mathbf{t} - \mathbf{s}_{i'}]_{\times} \mathbf{R}) \mathbf{Q}_i. \tag{53}$$

Denote

$$\tilde{\mathbf{A}}_k = \begin{bmatrix} \mathbf{A}_k & \mathbf{0}_{2 \times 1} \\ \mathbf{0}_{1 \times 2} & 1 \end{bmatrix}. \tag{54}$$

Then these constraints can be reformulated as

$$-\left[\begin{array}{c} (\mathbf{Q}_{i'}^T \mathbf{x}_k' \times \mathbf{R} \mathbf{Q}_i \mathbf{x}_k)^T \\ (\mathbf{Q}_{i'}^T \mathbf{x}_k' \times \mathbf{R} \mathbf{c}_1 + \mathbf{a}_1 \times \mathbf{R} \mathbf{Q}_i \mathbf{x}_k)^T \\ (\mathbf{Q}_{i'}^T \mathbf{x}_k' \times \mathbf{R} \mathbf{c}_2 + \mathbf{a}_2 \times \mathbf{R} \mathbf{Q}_i \mathbf{x}_k)^T \end{array} \right] \begin{bmatrix} \mathbf{t} \\ 1 \end{bmatrix} = \mathbf{0}, \tag{55}$$

where \mathbf{c}_i is the i -th column of \mathbf{Q}_i , \mathbf{a}_i is the i -th row of $\tilde{\mathbf{A}}_k^T \mathbf{Q}_{i'}$, and $\mathbf{o}_i(\mathbf{R})$ includes all terms depending on \mathbf{R} .

Proof. Equation (52a) can be reformulated as

$$\begin{aligned}
& \mathbf{x}_k'^T \mathbf{E}_k \mathbf{x}_k \\
& = \mathbf{x}_k'^T (\mathbf{Q}_{i'}^T [\mathbf{t}]_{\times} \mathbf{R} \mathbf{Q}_i) \mathbf{x}_k + \mathbf{o}_1(\mathbf{R}) \\
& = (\mathbf{Q}_{i'}^T \mathbf{x}_k')^T [\mathbf{t}]_{\times} \mathbf{R} (\mathbf{Q}_i \mathbf{x}_k) + \mathbf{o}_1(\mathbf{R}). \tag{56}
\end{aligned}$$

The expression in Eq. (52b) can be reformulated as

$$\begin{aligned}
& (\mathbf{E}_k^T \mathbf{x}_k') + \tilde{\mathbf{A}}_k^T (\mathbf{E}_k \mathbf{x}_k) \\
& = (\mathbf{Q}_{i'}^T [\mathbf{t}]_{\times} \mathbf{R} \mathbf{Q}_i)^T \mathbf{x}_k' + \tilde{\mathbf{A}}_k^T (\mathbf{Q}_{i'}^T [\mathbf{t}]_{\times} \mathbf{R} \mathbf{Q}_i) \mathbf{x}_k + \mathbf{o}_2(\mathbf{R}) \\
& = \mathbf{Q}_i^T ([\mathbf{t}]_{\times} \mathbf{R})^T \mathbf{Q}_{i'}^T \mathbf{x}_k' + \tilde{\mathbf{A}}_k^T \mathbf{Q}_{i'}^T ([\mathbf{t}]_{\times} \mathbf{R}) \mathbf{Q}_i \mathbf{x}_k + \mathbf{o}_2(\mathbf{R}) \tag{57}
\end{aligned}$$

where $\mathbf{o}_2(\mathbf{R})$ includes all terms depending on \mathbf{R} .

Similar to the derivation in Lemma 4, Eqs. (52a)(52b) can be reformulated as

$$-\begin{bmatrix} (\mathbf{Q}_{i'}\mathbf{x}'_k \times \mathbf{R}\mathbf{Q}_i\mathbf{x}_k)^T & o_1(\mathbf{R}) \\ (\mathbf{Q}_{i'}\mathbf{x}'_k \times \mathbf{R}\mathbf{c}_1 + \mathbf{a}_1 \times \mathbf{R}\mathbf{Q}_i\mathbf{x}_k)^T & [\mathbf{o}_2(\mathbf{R})]_1 \\ (\mathbf{Q}_{i'}\mathbf{x}'_k \times \mathbf{R}\mathbf{c}_2 + \mathbf{a}_2 \times \mathbf{R}\mathbf{Q}_i\mathbf{x}_k)^T & [\mathbf{o}_2(\mathbf{R})]_2 \end{bmatrix} \begin{bmatrix} \mathbf{t} \\ 1 \end{bmatrix} = \mathbf{0}, \quad (58)$$

where \mathbf{c}_i is the i -th column of $\mathbf{Q}_{i'}$, and \mathbf{a}_i is the i -th row of $\tilde{\mathbf{A}}_k^T \mathbf{Q}_{i'}$. \square

Theorem 4. Suppose \mathbf{N} is an arbitrary 4×4 submatrix of \mathbf{M} or an arbitrary 3×3 submatrix of the first three columns of \mathbf{M} , the polynomial $\det(\mathbf{N})$ has a factor $q_x^2 + q_y^2 + q_z^2 + 1$.

Proof. Denote

$$\mathbf{Q} = (q_x^2 + q_y^2 + q_z^2 + 1)\mathbf{R} \\ = \begin{bmatrix} 1 + q_x^2 - q_y^2 - q_z^2 & 2q_xq_y - 2q_z & 2q_y + 2q_xq_z \\ 2q_xq_y + 2q_z & 1 - q_x^2 + q_y^2 - q_z^2 & 2q_yq_z - 2q_x \\ 2q_xq_z - 2q_y & 2q_x + 2q_yq_z & 1 - q_x^2 - q_y^2 + q_z^2 \end{bmatrix}, \quad (59)$$

It can be verified that $\mathbf{Q}\mathbf{Q}^T = s^2\mathbf{I}$ with $s = q_x^2 + q_y^2 + q_z^2 + 1$.

Recall that \mathbf{M} is composed of constraints from two affine correspondences. According to Lemma 5, the constraints has the form of Eq. (55). So \mathbf{M} has a form of

$$\mathbf{M} = \begin{bmatrix} (\mathbf{a}_1 \times \mathbf{Q}\mathbf{b}_1 + \mathbf{c}_1 \times \mathbf{Q}\mathbf{d}_1)^T & o_1(\mathbf{Q}) \\ (\mathbf{a}_2 \times \mathbf{Q}\mathbf{b}_2 + \mathbf{c}_2 \times \mathbf{Q}\mathbf{d}_2)^T & o_2(\mathbf{Q}) \\ (\mathbf{a}_3 \times \mathbf{Q}\mathbf{b}_3 + \mathbf{c}_3 \times \mathbf{Q}\mathbf{d}_3)^T & o_3(\mathbf{Q}) \\ (\mathbf{a}_4 \times \mathbf{Q}\mathbf{b}_4 + \mathbf{c}_4 \times \mathbf{Q}\mathbf{d}_4)^T & o_4(\mathbf{Q}) \\ (\mathbf{a}_5 \times \mathbf{Q}\mathbf{b}_5 + \mathbf{c}_5 \times \mathbf{Q}\mathbf{d}_5)^T & o_5(\mathbf{Q}) \\ (\mathbf{a}_6 \times \mathbf{Q}\mathbf{b}_6 + \mathbf{c}_6 \times \mathbf{Q}\mathbf{d}_6)^T & o_6(\mathbf{Q}) \end{bmatrix}. \quad (60)$$

Note that \mathbf{Q} instead of \mathbf{R} appears in this matrix. The reason is that the scale factor $\frac{1}{q_x^2 + q_y^2 + q_z^2 + 1}$ is ignored during the construction of the equation system. In Eq. (60), the first three columns of coefficient matrix has the form of Eq. (41). Lemma 1 can be used directly. Thus we prove that the proposition is correct when \mathbf{N} is an arbitrary 3×3 submatrix of the first three columns of \mathbf{M} .

Next, we prove that the proposition is correct when \mathbf{N} is an arbitrary 4×4 submatrix of \mathbf{M} . The determinant can be calculated by the Laplace expansion along the fourth column, and it is the summation of each entry in the fourth column multiplied with the corresponding cofactor. Note that we have proved there is a factor $q_x^2 + q_y^2 + q_z^2 + 1$ for the determinant of an arbitrary 3×3 submatrix from the first three columns of \mathbf{M} . Then any cofactor has the factor $q_x^2 + q_y^2 + q_z^2 + 1$. \square

A.4 Proof of Theorem 5

Theorem 5. For non-degenerate cases, $\text{rank}(\mathbf{N}) = 2, \forall \mathbf{N} \in \mathcal{S}$. By Matlab syntax, \mathcal{S} is a set whose elements satisfying $\mathbf{N} = \tilde{\mathbf{M}}([k_1, k_2, k_3], 1 : 3)$, where k_1 -th, k_2 -th, and k_3 -th PCs are captured by the same perspective cameras across two views and $k_1 < k_2 < k_3$.

Proof. Let us investigate an arbitrary element in \mathcal{S} . Denote it is the k -th element \mathbf{N}_k in \mathcal{S} . The extrinsic parameter of the related perspective camera in view 1 is $[\mathbf{Q}_i|\mathbf{s}_i]$, and the extrinsic parameter of the related perspective camera in view 2 is $[\mathbf{Q}_{i'}|\mathbf{s}_{i'}]$.

First we prove that $\text{rank}(\mathbf{N}_k) \leq 2$. To achieve this goal, we need to prove that the null space of \mathbf{N}_k is not empty. Since k_1 -th, k_2 -th, and k_3 -th PCs are captured by the same perspective cameras across two views, their related essential matrices are the same. According to Eq. (30), the essential matrix is

$$\mathbf{E}_k = \mathbf{Q}_{i'}^T [\mathbf{t} + \mathbf{R}\mathbf{s}_i - \mathbf{s}_{i'}]_{\times} \mathbf{R}\mathbf{Q}_i. \quad (61)$$

Denote

$$\bar{\mathbf{t}} \triangleq \mathbf{t} + \mathbf{R}\mathbf{s}_i - \mathbf{s}_{i'}, \quad (62)$$

then we have

$$\mathbf{E}_k = \mathbf{Q}_{i'}^T [\bar{\mathbf{t}}]_{\times} \mathbf{R}\mathbf{Q}_i. \quad (63)$$

Substituting Eq. (63) into Eq. (29), we obtain three equations for the 3PCs. Each monomial in these three equations is linear with one entry of vector $\bar{\mathbf{t}}$, and there is no constant term. Thus these equations can be formulated as

$$\frac{1}{q_x^2 + q_y^2 + q_z^2 + 1} \mathbf{A}_k \bar{\mathbf{t}} = \mathbf{0}, \quad (64)$$

$$\Rightarrow \mathbf{A}_k(\mathbf{t} + \mathbf{R}\mathbf{s}_i - \mathbf{s}_{i'}) = \mathbf{0}, \quad (65)$$

$$\Rightarrow [\mathbf{A}_k \quad \mathbf{A}_k(\mathbf{R}\mathbf{s}_i - \mathbf{s}_{i'})] \begin{bmatrix} \mathbf{t} \\ 1 \end{bmatrix} = \mathbf{0}. \quad (66)$$

By comparing the construction procedure of Eq. (31) and Eq. (66), we can see that

$$\mathbf{A}_k = \widehat{\mathbf{M}}([k_1, k_2, k_3], 1 : 3) = \mathbf{N}_k. \quad (67)$$

Substituting this equation into Eq. (64), we can see that the null space of \mathbf{N}_k is not empty.

Next we prove that $\text{rank}(\mathbf{N}_k) \geq 2$. We achieve this goal using proof by contradiction. If $\text{rank}(\mathbf{N}_k) \leq 1$, then $\text{rank}(\widehat{\mathbf{M}}([k_1, k_2, k_3], 1 : 4)) \leq 2$ considering that $\widehat{\mathbf{M}}([k_1, k_2, k_3], 1 : 4)$ has one more column than \mathbf{N}_k . This means the three ACs provides at most two independent constraints for the relative pose. This cannot be true for non-degenerate cases, so the assumption that $\text{rank}(\mathbf{N}_k) \leq 1$ is wrong. \square

APPENDIX B

NUMERICAL STABILITY IMPROVEMENT FOR 2AC+INTRA AND 6PT+INTRA

The numerical stability of 2AC+intra and 6pt+intra are more complicated than other cases. The GrevLex monomial orderings is exploited during solver generation which reads as follows: which is $q_x > q_y > q_z$. Under such an ordering, we found that when one of the following two conditions is satisfied, their solvers are numerically unstable. Condition 1: the z -coordinates of \mathbf{s}_1 and \mathbf{s}_2 are the same. Condition 2: the x - and y -coordinates of \mathbf{s}_1 and \mathbf{s}_2 are the same, i.e., $(\mathbf{s}_1)_{(1:2)} = (\mathbf{s}_2)_{(1:2)}$.

We developed a technique to improve the numerical stability of these two solvers. Our idea is to destroy the two conditions mentioned above by defining a new reference for the multi-camera system. The new reference is uniquely determined by satisfying the following two conditions. (i) Its origin is the middle point of two cameras in the two-camera rig. (ii) Two focal points of perspective cameras lie

on points $\frac{L}{2\sqrt{3}}[-1, -1, -1]^T$ and $\frac{L}{2\sqrt{3}}[1, 1, 1]^T$ in the new reference, respectively. Here $L = \|s_1 - s_2\|$ is the distance between two focal points of the two-camera rig. In this new reference, the two conditions causing numerical instability are destroyed as largely as possible. After the relative pose in the new reference is obtained, we convert the relative pose to the original reference. This technique is applied to 2AC+intra and 6pt+intra only since it slightly decreases the numerical stability for other cases and increases calculation.

B.1 Reference Transformation

We introduce more details about reference transformation. The coordinates of focal points in the original frame are s_1 and s_2 . We aim to define a new reference, in which these two points has coordinates $\frac{L}{2\sqrt{3}}[-1, -1, -1]^T$ and $\frac{L}{2\sqrt{3}}[1, 1, 1]^T$, respectively. Here $L = \|s_1 - s_2\|$ is the distance between two focal points of the two-camera rig.

Denote the unit direction vector connecting two focal points in the original frame and new frame as $\mathbf{a} = \frac{1}{L}(s_2 - s_1)$, $\mathbf{b} = \frac{1}{\sqrt{3}}[1, 1, 1]^T$, respectively. The rotation can be found by axis-angle parameterization. Denote

$$\mathbf{v} = \frac{\mathbf{a} \times \mathbf{b}}{\|\mathbf{a} \times \mathbf{b}\|}, \quad (68)$$

$$s = \|\mathbf{a} \times \mathbf{b}\|, \quad (69)$$

$$c = \mathbf{a} \cdot \mathbf{b}. \quad (70)$$

Here \mathbf{v} is the rotation axis. s and c are sine and cosine of the rotation angle, respectively. According to Rodrigues' rotation formula, the transformation rotation is

$$\mathbf{R}_0 = \mathbf{I} + s[\mathbf{v}]_{\times} + (1 - c)[\mathbf{v}]_{\times}^2. \quad (71)$$

For the middle point of the line segment between two focal points, its coordinates are $\frac{1}{2}(s_1 + s_2)$ and $[0, 0, 0]^T$ in the original frame and new frame, respectively. Thus the translation is

$$\mathbf{t}_0 = -\frac{1}{2}\mathbf{R}_0(s_1 + s_2). \quad (72)$$

The Matlab code is listed below.

```
function [R, t] = find_optimal_transformation3(s1, s2)
% Input
% s1 and s2: focal points of the perspective cameras
% in the original frame
% Output
% R and t satisfy: the direction of R*s1+t and R*s2+t
% are [-1;-1;-1] and [1;1;1], respectively.
m = (s1+s2)/2;
a = s2-s1;
a = a/norm(a);
b = [1;1;1]/sqrt(3);
v = cross(a,b);
s = norm(v);
if (s>1e-10)
    v = v/s;
    SV = [0 -v(3) v(2); v(3) 0 -v(1); -v(2) v(1) 0];
    R = eye(3) + SV*s + SV*2*(1-dot(a,b));
else
    R = eye(3);
end
t = -R*m;
```

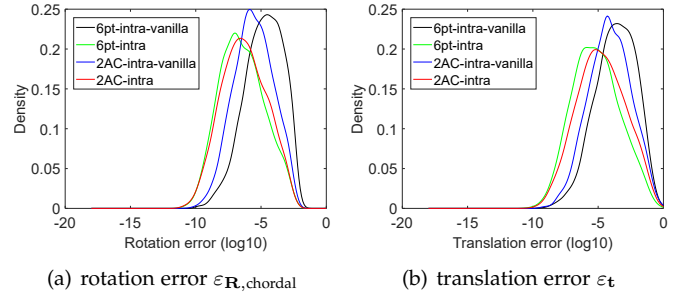


Fig. 10. Probability density functions over pose estimation errors on noise-free observations using reference transformation. The horizontal axis represents the \log_{10} errors and the vertical axis represents the density.

B.2 Experiments

Fig. 10 reports the numerical stability of the solvers on noise-free observations. Vanilla version means using the solvers without reference transformation. The proposed reference transformation can reduce the numerical errors significantly. For 6pt+intra, the mode of $\varepsilon_{\mathbf{R}, \text{chordal}}$ is decreased from $10^{-4.5}$ to 10^{-7} , and the mode of ε_t is decreased from $10^{-3.5}$ to $10^{-5.9}$. For 2AC+intra, the mode of $\varepsilon_{\mathbf{R}, \text{chordal}}$ is decreased from $10^{-5.9}$ to $10^{-6.6}$, and the mode of ε_t is decreased from $10^{-4.3}$ to $10^{-5.2}$.

APPENDIX C

EXTENSIONS OF RELATIVE POSE FROM AFFINE CORRESPONDENCES

The minimal solver generation framework in this paper has great potential to solve many other relative pose estimation tasks. In this section, we extend this idea to many other configurations.

C.1 Known Rotation Angle

When the rotation angle is known, the DOF of rotation can be reduced by one. There are minimal solvers for single cameras [41], [42], [43] or multi-camera systems [43] using PCs. Our method can be easily extended to deal with known rotation angle cases.

The known rotation angle prior imposes one constraint for rotation. Suppose the known rotation angle is θ . By exploiting the relation between quaternion and axis-angle representation, a constraint can be constructed. For Cayley and quaternion parameterizations, the constraints are

$$q_x^2 + q_y^2 + q_z^2 - \tan^2(\theta/2) = 0, \quad (73)$$

TABLE 7

Minimal solvers for 5DOF relative pose estimation of single cameras. “+ka” represents rotation angle is known. “+f” represents that the focal length is unknown.

configuration	#sol	template	#sym.	action matrix
2ac+cayl+mono	20	36×56	0	20×20
2ac+cayl+mono+ka	20	36×56	0	20×20
2ac+cayl+mono+f	60	213×243	1	30×30
2ac+cayl+mono+ka+f	80	300×340	1	40×40

TABLE 8

Minimal solvers for relative pose estimation with a known rotation angle for multi-camera systems. “+ka” represents rotation angle is known. “+f” represents that all focal lengths are unknown.

configuration	equations \mathcal{E}_1		equations $\mathcal{E}_1 + \mathcal{E}_2$	
	#sol	template	#sol	template
2ac+cayl+(case 1 ~ 5)+ka	44	120×164	36	84×120
2ac+cayl+(case 6)+ka	42	98×164	36	104×164
2ac+cayl+(case 7)+ka	44	120×164	36	84×120
2ac+cayl+(case 1 ~ 2)+ka+f	352	2307×2659	288	1657×1945
2ac+cayl+(case 3)+ka+f	352	1837×2197	288	1648×1945
2ac+cayl+(case 4)+ka+f	324	2632×2998	276	2113×2407
2ac+cayl+(case 5)+ka+f	322	3165×3544	274	2648×2953
2ac+cayl+(case 6)+ka+f	328	2796×3282	280	2503×3064
2ac+cayl+(case 7)+ka+f	1-dim	—	288	2430×2819

and

$$q_x^2 + q_y^2 + q_z^2 - \tan^2(\theta/2)q_w^2 = 0, \quad (74)$$

respectively. Note that 2 ACs provide 6 independent constraints, and the known rotation angle case has 4 and 5 unknowns for a single camera and a multi-camera system, respectively. To construct a minimal configuration, we remove the excess constraints. For a single camera, the minimal configuration becomes 1AC+1PC.

For single camera systems, the solver has 20 solutions and the elimination template is 36×56 , see Table 7. For multi-camera systems, the statistics of the resulted solvers are shown in Table 8. The solvers have 36 solutions.

C.2 Relative Pose and Focal Length Problem

Our method can also be extended to semi-calibrated cameras. To simplify the problem, we assume only focal length is unknown. For multi-camera systems, we further assume all perspective cameras have the same focal length. Let f be the unknown focal length of the perspective cameras in a multiple camera system. The intrinsic matrix becomes

$$\mathbf{K}^{-1} = \begin{bmatrix} w & 0 & 0 \\ 0 & w & 0 \\ 0 & 0 & 1 \end{bmatrix}, \quad (75)$$

where $w = 1/f$.

Denote the k -th AC as $(\hat{\mathbf{x}}_k, \hat{\mathbf{x}}'_k, \mathbf{A}_k)$, where $\hat{\mathbf{x}}_k$ and $\hat{\mathbf{x}}'_k$ are the homogeneous coordinates in image plane for the first and the second views, respectively.

$$\mathbf{x}_k = \mathbf{K}^{-1}\hat{\mathbf{x}}_k, \quad \mathbf{x}'_k = \mathbf{K}^{-1}\hat{\mathbf{x}}'_k. \quad (76)$$

For a single camera, the three equations induced by one AC becomes

$$\begin{cases} \hat{\mathbf{x}}_k^T \mathbf{K}^{-T} \mathbf{E} \mathbf{K}^{-1} \hat{\mathbf{x}}_k = 0 \\ (\mathbf{E}^T \mathbf{K}^{-1} \hat{\mathbf{x}}'_k)_{(1:2)} = -\mathbf{A}_k^T (\mathbf{E} \mathbf{K}^{-1} \hat{\mathbf{x}}_k)_{(1:2)} \end{cases} \quad (77a)$$

$$(77b)$$

There are 5DOF unknown pose and one unknown inverse focal length in this equation system. Thus the setting of two ACs is a minimal configuration. There is a symmetry in this equations system: if $\{q_x, q_y, q_z, w\}$ is a solution, $\{-q_x, -q_y, q_z, -w\}$ is also a solution. In addition, an inequality $w \neq 0$ should be explicitly considered. Otherwise, there is one-dimensional extraneous roots. We consider this inequality by saturation method [69]. By the hidden variable

TABLE 9

Runtime comparison of solvers for single cameras (unit: μs).

method	5pt-Nister [5]	2AC-Barath [18]	2AC-mono
mean time	5.5	11.0	140.2

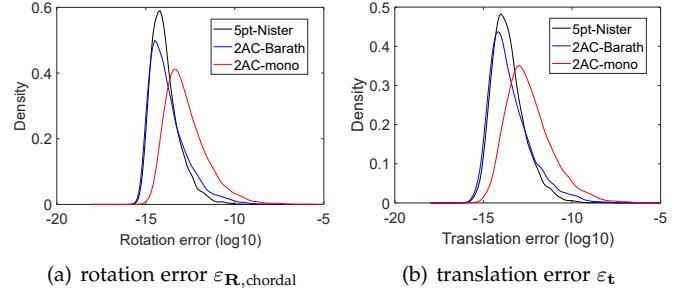


Fig. 11. Probability density functions over pose estimation errors on noise-free observations for single cameras. The horizontal axis represents the \log_{10} errors and the vertical axis represents the density.

technique, we obtain a solver with 60 solutions. The elimination template is 213×243 and the action matrix is 30×30 , see Table 7.

For multi-camera systems, the solver can be constructed similarly. The minimal configuration is 2 ACs plus 1 PC, which has too many variants. To simplify the problem, we assume that the rotation angle is known, which makes 2AC being the minimal configuration. The statistics of the resulted solvers are shown in Table 8. It can be seen that both the solution number and elimination template are large. As a result, the solvers are neither efficient nor numerical stable. These results suggest that we should further reduce problem complexity to obtain a practical solver. For example, we may further reduce DOF of the relative pose by exploiting the known rotation axis prior or planar motion prior, or we can reduce the order of the polynomial equation system by assuming that only part of focal lengths is unknown. It is straightforward to obtain solvers for these cases using our framework.

APPENDIX D EXPERIMENTS

D.1 Experiments for Single Cameras

In this paper, we obtain a minimal solver for single-cameras as a side product. The purpose of the following experiments is not to outperform the state-of-the-art method [18]. Instead, we illustrate that the obtained solver is practical.

For single cameras, the proposed solver is referred to as 2AC-mono. The proposed solvers are compared with state-of-the-art solvers including 5pt-Nister [5] and 2AC-Barath [18]. All the solvers are implemented in C++. The code of 5pt-Nister is provided by the PoseLib², and 2AC-Barath is publicly available from the code of [20].

Table 9 shows the average runtime of the solvers over 10,000 runs for single cameras. Two methods based on 2AC are more efficient than 5pt-Nister method. 2AC-Barath

2. <https://github.com/vlarsson/PoseLib>

takes $11\mu s$ on average. The proposed 2AC-mono takes about 0.14 milliseconds, which is one order magnitude slower than 2AC-Barath. Still, it is applicable for common scenarios and provides another option for this task.

Figure 11 reports the numerical stability of the solvers on noise-free observations. The procedure is repeated 10,000 times. The empirical probability density functions are plotted as the function of the \log_{10} estimated errors $\varepsilon_{\mathbf{R}}$ and $\varepsilon_{\mathbf{t}}$. It can be seen that 2AC-Barath and 5pt-Nister have nearly the same numerical stability. The proposed 2AC-mono has worse numerical stability than them. Still, it is applicable for practical applications since both the rotation error and translation error are below 1×10^{-8} , and the modes of the rotation error and translation error are about 1×10^{-13} .